Multipole analysis of $p(\vec{e}, e'\vec{p})\pi^0$ response functions at $Q^2 = 1$ (GeV/c)^2 across the $\Delta(1232)$ resonance

Internal Report to the JLab E91-011 Collaboration

J. J. Kelly[1]

[1]*Department of Physics, University of Maryland, College Park, Maryland 20742, USA*

(Dated: March 23, 2005; revised July 18, 2005)

We have performed a multipole analysis of differential cross section, beam analyzing power, and recoil-polarization response functions for the $p(\vec{e}, e'\vec{p})\pi^0$ reaction at $Q^2 = 1$ (GeV/c)^2 in 10 bins of $1.17 \le W \le 1.35$ GeV across the $\Delta(1232)$ resonance. Pseudodata tests indicate that a dipole parametrization of the Q^2 dependence of response functions is sufficient to project binned data to central kinematics. Our standard analysis uses a pseudovector Born baseline and varies all $\ell \le 1$ amplitudes except Im M_{1-} plus Re 2− amplitudes. Fitted multipole amplitudes and quadrupole amplitudes are nearly independent of the choice of baseline model and display smooth W dependences. Uncertainties due to systematic errors in response functions or the kinematic correction are generally small compared with statistical or fitting uncertainties. Using a parabolic fit to the energy dependence, we obtain Re $(S_{1+}^{(p\pi^0)}/M_{1+}^{(p\pi^0)}) = -(6.61 \pm 0.18)\%$ and Re $(E_{1+}^{(p\pi^0)}/M_{1+}^{(p\pi^0)}) = -(2.87 \pm 0.19)\%$ at $W = M_\Delta = 1.232$ GeV and $Q^2 = 1.0$ (GeV/c)^2.

I. INTRODUCTION

This internal report presents some of the details for the multipole analysis of data for the differential cross section and recoil-polarization response functions for the $p(\vec{e}, e'\vec{p})\pi^0$ reaction at $Q^2 \sim 1$ (GeV/c)^2 across the $\Delta(1232)$ resonance that were obtained by the JLab e91011 collaboration. This report is updated periodically as the data analysis evolves. The final version of this report is intended as a supplement to a Phys. Rev. C paper because there are far too many figures for a typical journal paper. Details of the conventions for response functions are presented in the PRC draft [1] and will not be repeated here. Details of the fitting procedures may be found in Ref. [2].

In Sec. II we evaluate the sensitivity of the multipole analysis to deviations between acceptance-averaged and central values of (W, Q^2). In Sec. III we present a multipole analysis based upon a Born baseline model and determine the optimum set of free parameters. In Sec. IV we evaluate the sensitivity of multipole amplitudes to the choice of baseline model. Systematic uncertainties are evaluated in Sec. V. The fitted multipole amplitudes and quadrupole ratios are discussed in Sec. VI. Our conclusions are summarized in Sec. VII.

II. SENSITIVITY TO BIN CENTERING

Multipole amplitudes are functions of (W, Q^2), but the acceptance averaged $(\overline{W}, \overline{Q^2})$ depend upon $x = \cos\theta_\pi^{(cm)}$. Consequently, multipole amplitudes fitted to angular distributions can be distorted by the variations of $(\overline{W}, \overline{Q^2})$ with x. Two methods for compensating for such distortions were studied in Ref. [3] using pseudodata and we chose the multiplicative method for the final analysis. This method assumes that the dominant effect is the dependence of $\overline{Q^2}$ upon x and that all response functions share a common form factor. Thus, projection to the nominal Q^2 is performed according to

$$R(W, Q^2, \bar{x}) = R(\overline{W}, \overline{Q^2}, \bar{x}) \left(G(Q^2)/G(\overline{Q^2}) \right)^2 \tag{1}$$

where we approximate $G(Q^2)$ by the usual dipole form factor, $G_D(Q^2) = (1 + Q^2/\Lambda^2)^{-2}$ with $\Lambda^2 = 0.71$ (GeV/c)^2. This multiplicative procedure does not compensate for variations of $\overline{W}$, but those variations are much smaller than those for $\overline{Q^2}$. Systematic uncertainties in multipole amplitudes due to variations of $G(Q^2)$ are estimated in Sec. V.

The effects of bin-centering corrections are illustrated in Figs. 1-10 for response functions and Figs. 11-13 for multipoles. The fits were based upon the Born baseline model and vary all $\ell \le 1$ amplitudes plus the real parts of 2− amplitudes. The sensitivity of these fits to the truncation scheme and to the choice of baseline model will be explored more carefully in Sections III and IV. Note that kinematical corrections were not applied to the cross section data from which unpolarized response functions were extracted — the data for differential cross sections already includes corrections that project to central kinematics. The effect of kinematical corrections on recoil-polarization response functions is generally small, though bin centering does reduce nonstatistical scatter and improves χ^2_ν. The effects on multipole amplitudes are largest in the 1+ partial wave where centering tends to shift fitted amplitudes toward the

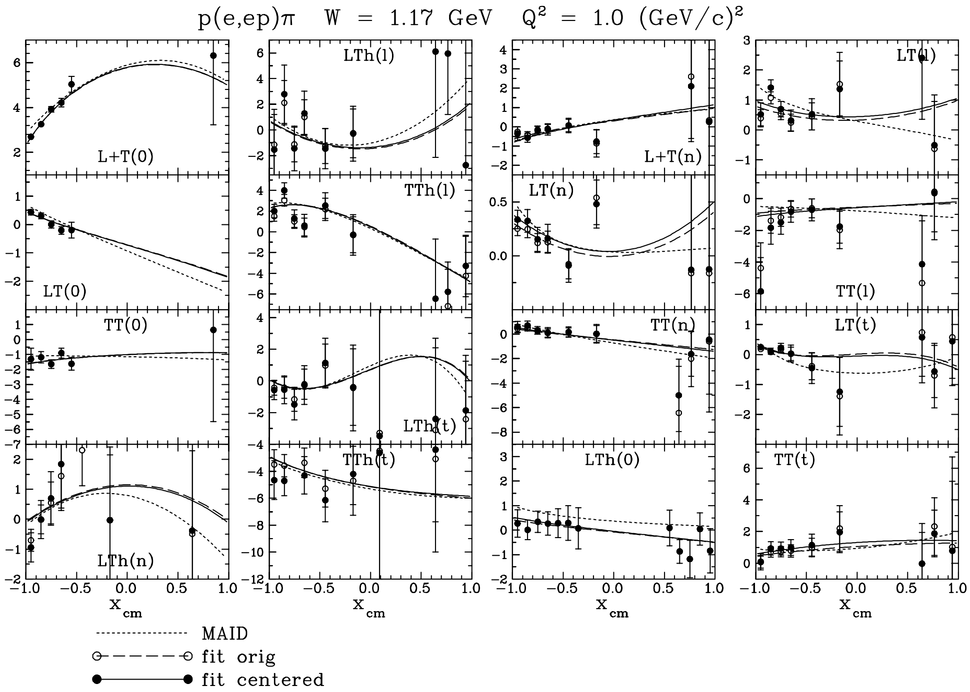

FIG. 1: Sensitivity of multipole fits for $W = 1.17$ GeV at $Q^2 = 1.0$ (GeV/c)^2 to bin centering. The dashed curves fit data (open circles) without adjustments for Q^2 variations while solid curves fit data (filled circles) with adjustments based upon MAID2003. The MAID2003 predictions are shown by dotted curves.

model curves and smoothens the W dependencies. The corresponding effects on nondominant partial waves are much smaller and have no effect upon the qualitative conclusions.

Finally, Fig. 14 shows the sensitivity of fitted quadrupole ratios to multiplicative kinematical corrections. For EMR there is a slight reduction in magnitude from $-(3.04 \pm 0.23)\%$ to $-(2.72 \pm 0.20)\%$, while SMR changes from $-(6.64 \pm 0.33)\%$ to $-(6.85 \pm 0.27)\%$ at $W = 1.23$ GeV. Both changes are about 1σ.

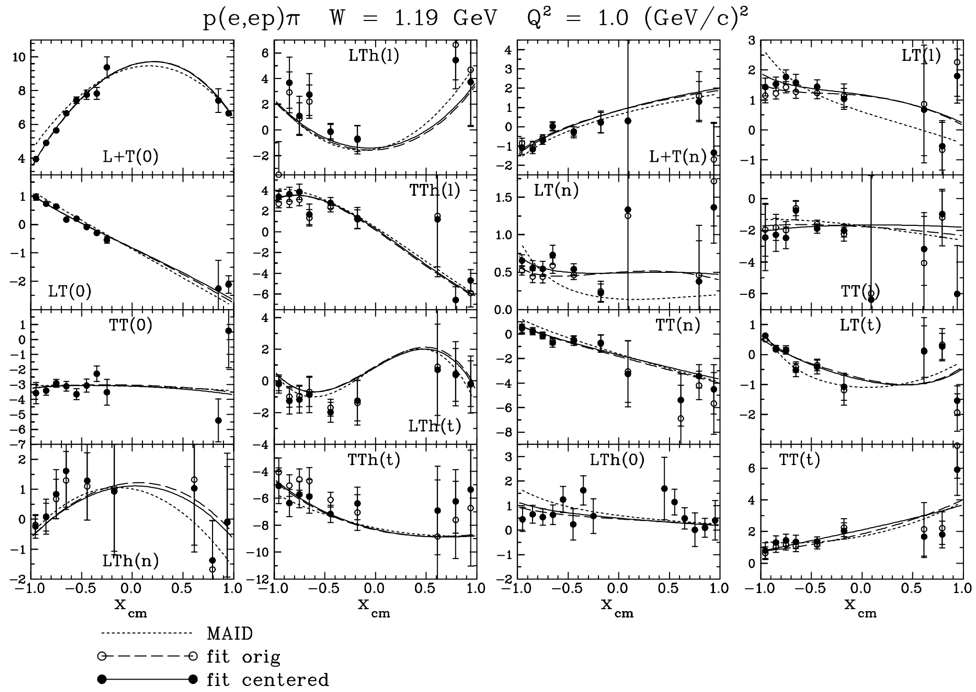

FIG. 2: Sensitivity of multipole fits for $W = 1.19$ GeV at $Q^2 = 1.0$ (GeV/c)^2 to bin centering. The dashed curves fit data (open circles) without adjustments for Q^2 variations while solid curves fit data (filled circles) with adjustments based upon MAID2003. The MAID2003 predictions are shown by dotted curves.

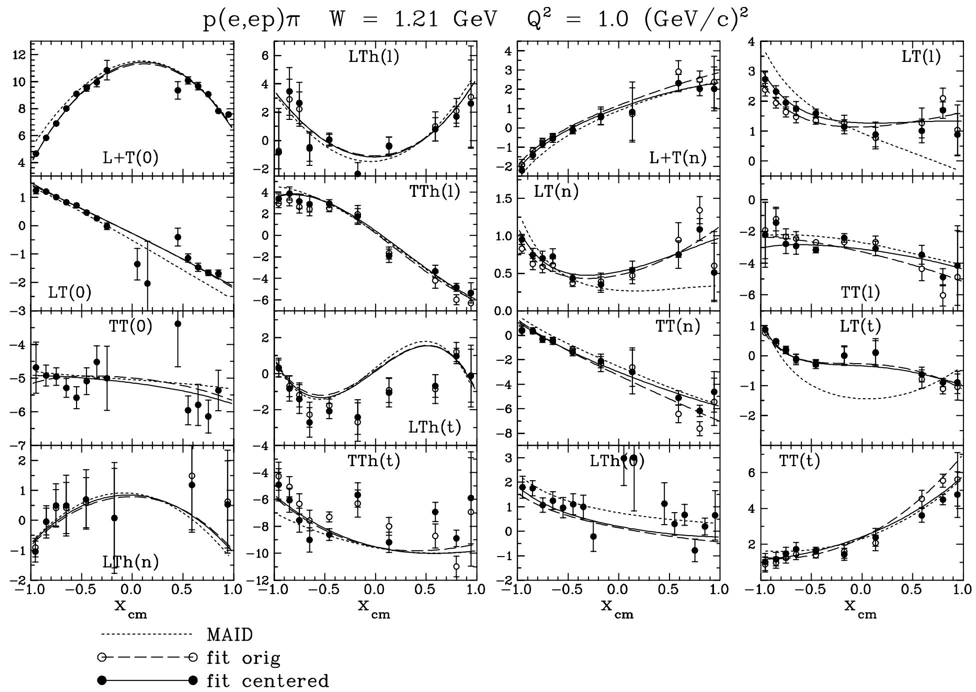

FIG. 3: Sensitivity of multipole fits for $W = 1.21$ GeV at $Q^2 = 1.0$ (GeV/c)^2 to bin centering. The dashed curves fit data (open circles) without adjustments for Q^2 variations while solid curves fit data (filled circles) with adjustments based upon MAID2003. The MAID2003 predictions are shown by dotted curves.

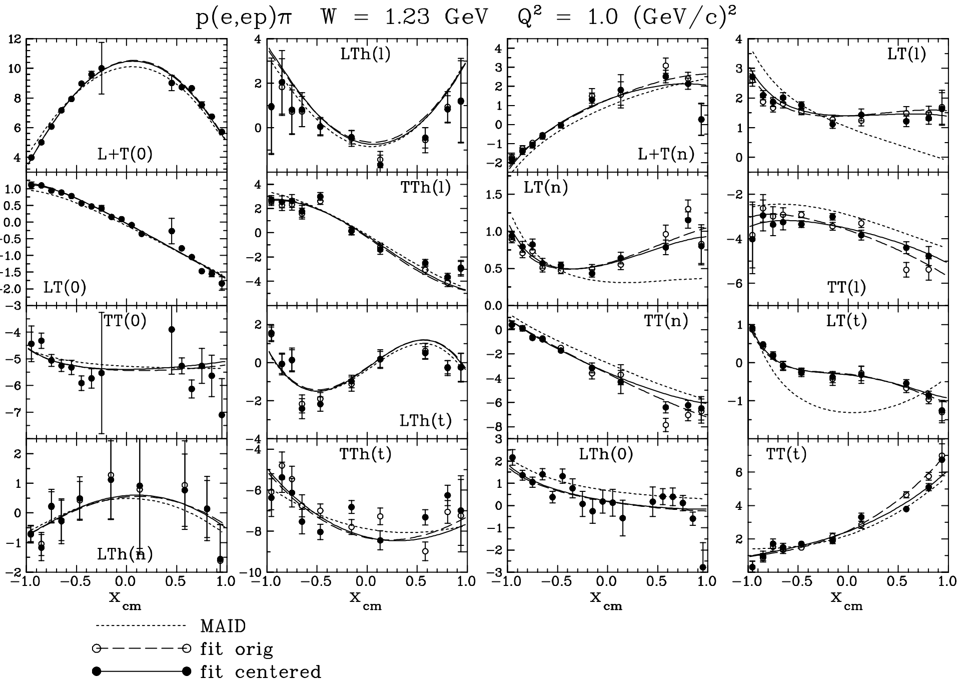

FIG. 4: Sensitivity of multipole fits for $W = 1.23$ GeV at $Q^2 = 1.0$ (GeV/c)^2 to bin centering. The dashed curves fit data (open circles) without adjustments for Q^2 variations while solid curves fit data (filled circles) with adjustments based upon MAID2003. The MAID2003 predictions are shown by dotted curves.

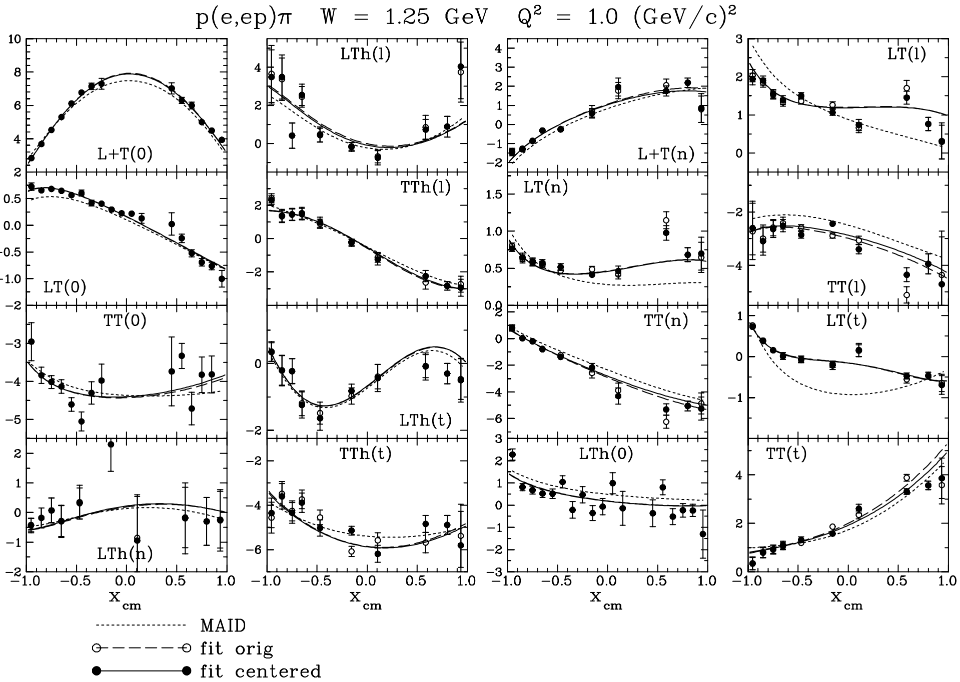

FIG. 5: Sensitivity of multipole fits for $W = 1.25$ GeV at $Q^2 = 1.0$ (GeV/c)^2 to bin centering. The dashed curves fit data (open circles) without adjustments for Q^2 variations while solid curves fit data (filled circles) with adjustments based upon MAID2003. The MAID2003 predictions are shown by dotted curves.

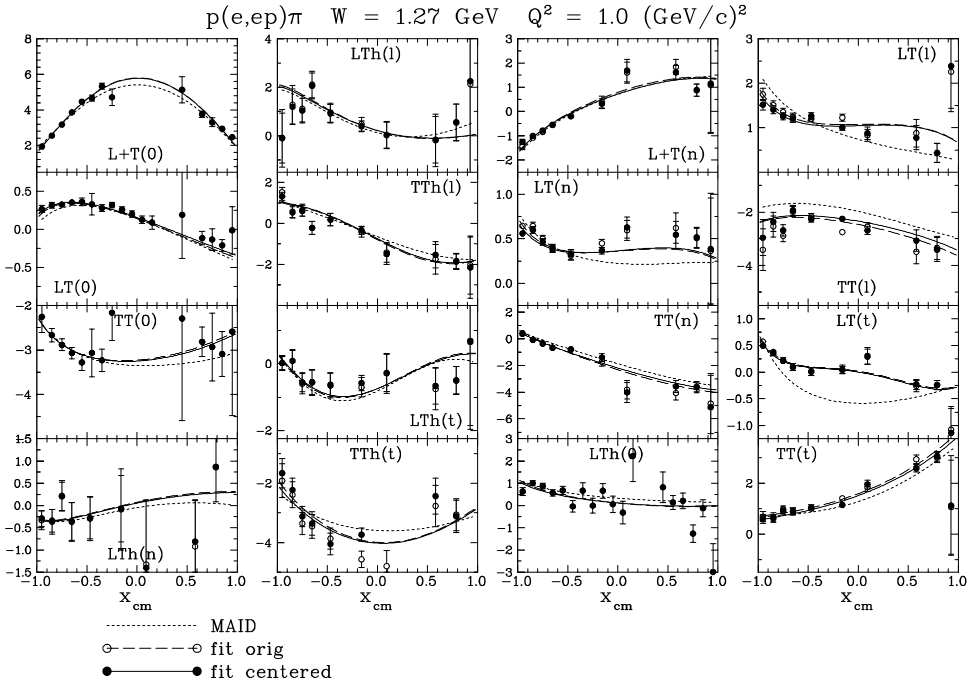

FIG. 6: Sensitivity of multipole fits for $W = 1.27$ GeV at $Q^2 = 1.0$ (GeV/c)^2 to bin centering. The dashed curves fit data (open circles) without adjustments for Q^2 variations while solid curves fit data (filled circles) with adjustments based upon MAID2003. The MAID2003 predictions are shown by dotted curves.

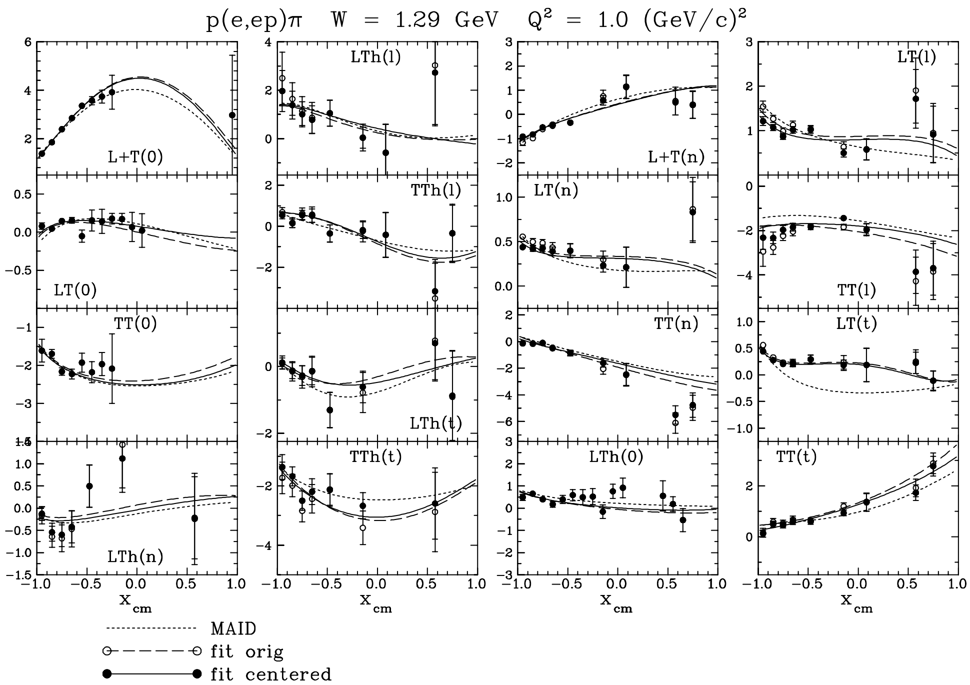

FIG. 7: Sensitivity of multipole fits for $W = 1.29$ GeV at $Q^2 = 1.0$ (GeV/c)^2 to bin centering. The dashed curves fit data (open circles) without adjustments for Q^2 variations while solid curves fit data (filled circles) with adjustments based upon MAID2003. The MAID2003 predictions are shown by dotted curves.

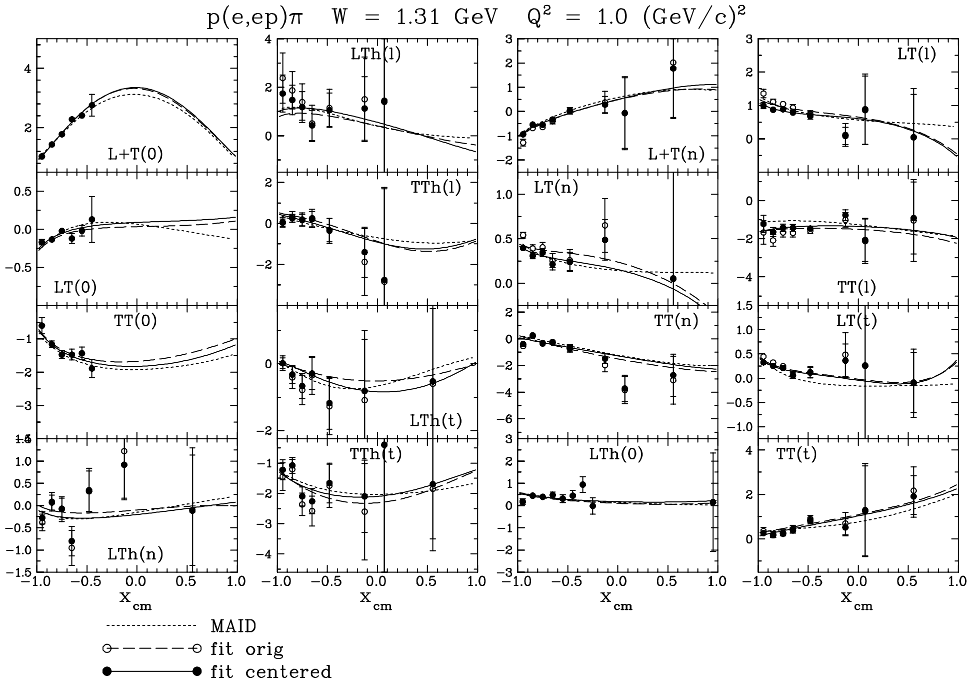

FIG. 8: Sensitivity of multipole fits for $W = 1.31$ GeV at $Q^2 = 1.0$ (GeV/c)^2 to bin centering. The dashed curves fit data (open circles) without adjustments for Q^2 variations while solid curves fit data (filled circles) with adjustments based upon MAID2003. The MAID2003 predictions are shown by dotted curves.

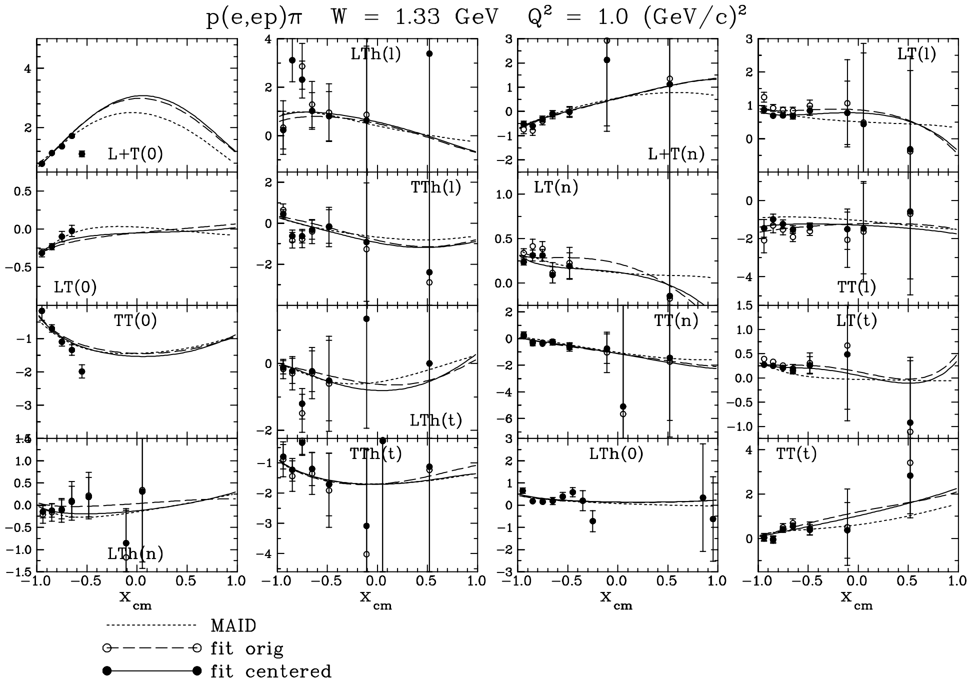

FIG. 9: Sensitivity of multipole fits for $W = 1.33$ GeV at $Q^2 = 1.0$ (GeV/c)^2 to bin centering. The dashed curves fit data (open circles) without adjustments for Q^2 variations while solid curves fit data (filled circles) with adjustments based upon MAID2003. The MAID2003 predictions are shown by dotted curves.

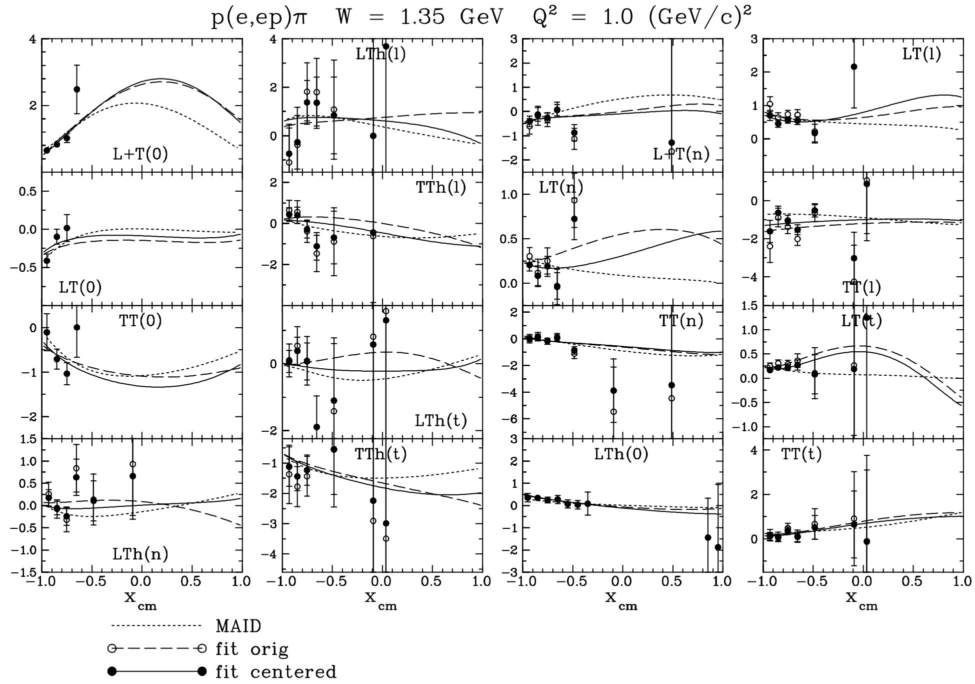

FIG. 10: Sensitivity of multipole fits for $W = 1.35$ GeV at $Q^2 = 1.0$ (GeV/c)^2 to bin centering. The dashed curves fit data (open circles) without adjustments for Q^2 variations while solid curves fit data (filled circles) with adjustments based upon MAID2003. The MAID2003 predictions are shown by dotted curves.

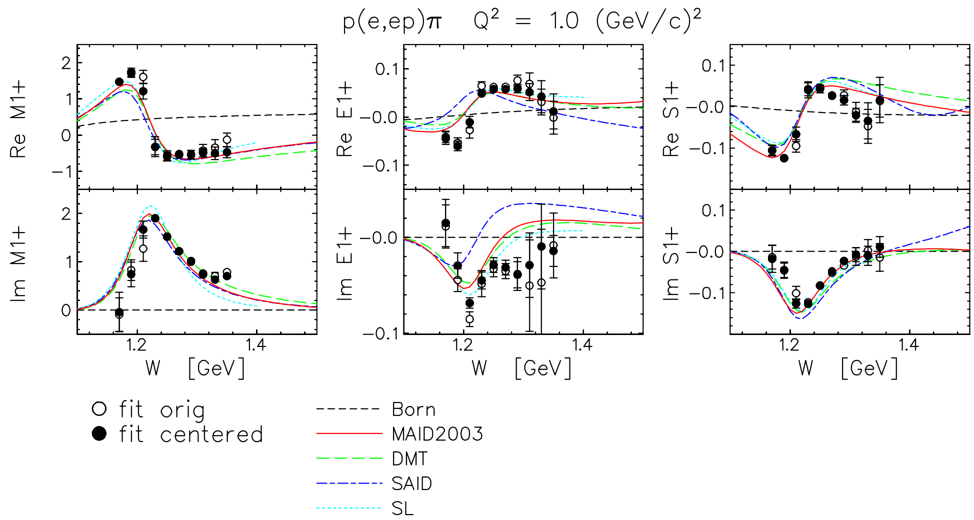

FIG. 11: Sensitivity of fitted multipole amplitudes to the corrections for Q^2 variations.

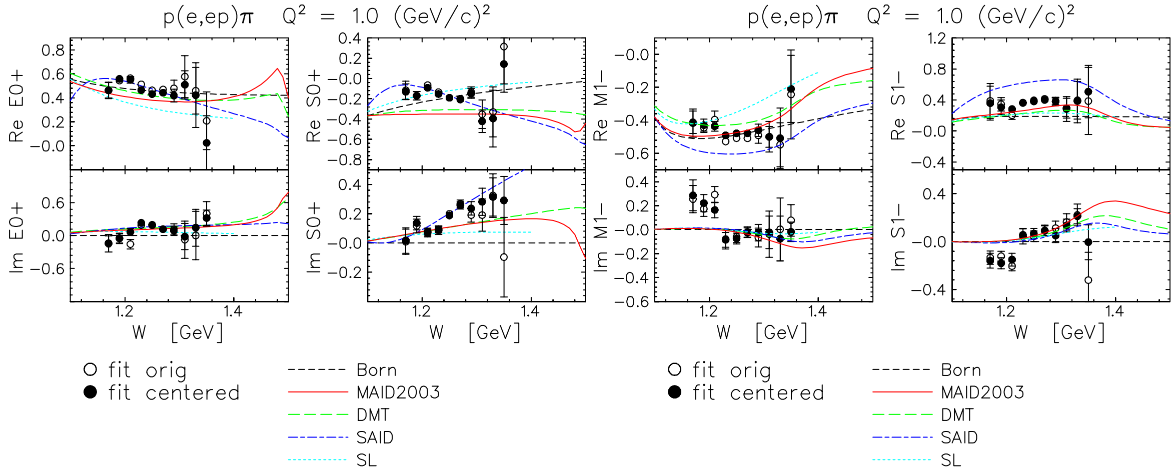

FIG. 12: Sensitivity of fitted multipole amplitudes to the corrections for Q^2 variations.

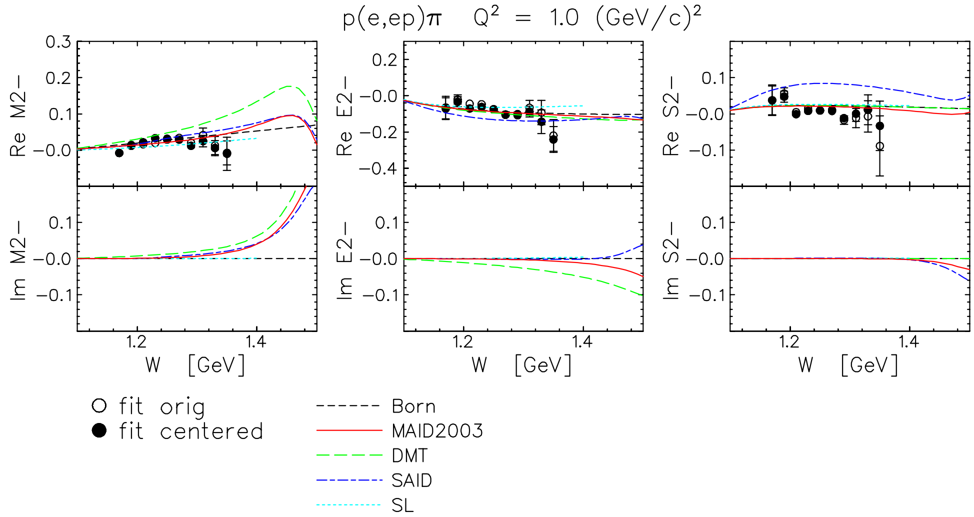

FIG. 13: Sensitivity of fitted multipole amplitudes to the corrections for Q^2 variations.

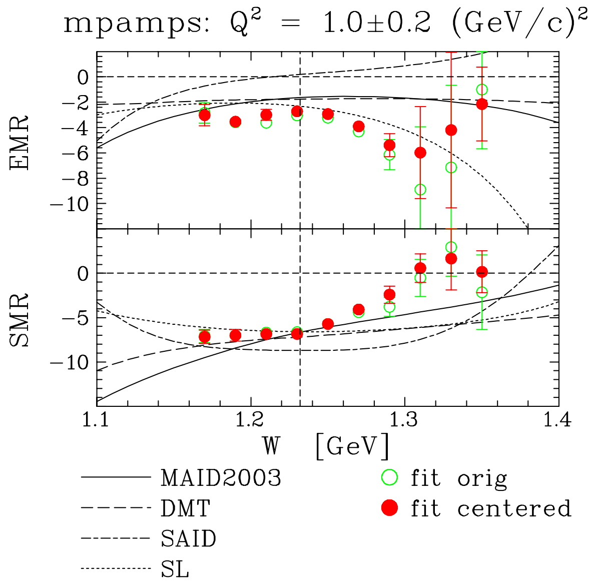

FIG. 14: Sensitivity of fitted quadrupole ratios to the corrections for Q^2 variations.

III. ANALYSIS USING BORN BASELINE

Fits using Born amplitudes for pseudovector coupling as the baseline model are shown in Figs. 15-24. Several fits were performed to determine the maximum number of parameters that can be extracted without flattening the χ^2 hypersurfaces too severely or encountering uncontrollable correlations among parameters. Dashed curves, designated *sp*, show fits that adjust real and imaginary parts of all s- and p-wave multipole amplitudes with higher partial waves constrained by the baseline model, here just real Born amplitudes without resonances. The fits designated *spd*3 also vary the real parts of $2-$ multipoles and are shown as blue dotted curves. Fits designated *spd* vary real and imaginary parts of all amplitudes with $\ell \leq 2$ and are shown as green dash-dotted curves. Finally, the fits designated "final" are similar to the *spd*3 fits except that Im M_{1-} is held at baseline, here zero, for reasons discussed below.

These figures show that fitting just the s- and p-wave amplitudes, with a Born background, is already sufficient to obtain a good description of these data. Although fitting d-wave amplitudes, or a subset thereof, sometimes provides modest reductions of χ^2, there is little systematic evidence that modification of d-wave or higher multipoles is really necessary. However, it is also clear that variation of all $\ell \leq 2$ amplitudes offers too much freedom — the oscillations in green dash-dotted curves for $W \geq 1.29$ GeV or $W \leq 1.19$ GeV are not needed to fit the data, are implausible in amplitude, and change too much from one W to the next.

The fitted multipole amplitudes are compared in Figs. 25-27 with several recent models [4–7]. In addition, the baseline Born amplitudes are shown by dashed curves. Note that all multipole amplitudes are real in this model and there are no resonances; therefore, the starting conditions are quite poor and large adjustments to the initial parameters are required to fit the data. Nevertheless, the fits describe the data well, the fitted parameters generally display smooth W dependencies, and the characteristic resonance profiles emerge in the $1+$ multipole amplitudes without coaching. Note that the *sp* and final fits began with baseline amplitudes but to improve stability the fits with more freedom began with the results of the final analysis. The uncertainties increase with the number of free parameters because the data do not adequately constrain multipoles for $\ell \geq 2$. Thus, we reject the full *spd* analysis because the uncertainties in its parameters are large and the resultant oscillations in calculated response functions are not warranted by the available data. The amplitudes and resulting fits for the other three analyses tend to be very similar except that there is a rather strong correlation between Im M_{1-} and Im S_{1-} for small W that results in fitted values of opposite sign that are substantially larger than model predictions for $W \leq 1.21$ GeV. This correlation also appears to affect imaginary parts of $1+$ amplitudes for $W = 1.17$ GeV. Evidently, the data for low W do not distinguish between Im M_{1-} and Im S_{1-} well enough to fit both simultaneously. Therefore, our final analysis eliminates Im M_{1-} because models tend to predict stronger Im S_{1-} amplitudes and the *sp* fit also produces rather small Im M_{1-} values. The "final" analysis varies both real and imaginary parts of S_{1-} and all $0+$ and $1+$ multipoles plus the real parts of M_{1-} and all $2-$ multipoles for a total of 16 free parameters for each (W, Q^2) bin. The uncertainties in fitted multipoles is reduced and the W dependencies are improved, especially for imaginary $1+$ amplitudes, upon elimination of this redundant parameter. Furthermore, Figs. 15-24 demonstrate that elimination of Im M_{1-} does not visibly reduce the quality of the fits to the data.

Figure 28 shows the sensitivity of fitted quadrupole ratios to the number of variable amplitudes and Table I lists SMR and EMR at $W = 1.23$ GeV for each truncation scheme. The *sp* fits provide smooth dependencies upon W and small parameter uncertainties based upon the covariance matrix. Increasing the parameter space to include real parts of $2-$ multipoles increases the uncertainties in fitted parameters slightly without producing any significant systematic changes in the fitted ratios; in fact, many of the previous points are obscured. However, expanding the parameter space to include all amplitudes with $\ell \leq 2$ offers the fit more parameters than the data can determine; consequently the scatter and error bars increase significantly. Interestingly, the estimated uncertainty in SMR is smaller for the last line than for the *sp* fit even though the former has more free parameters than the latter. Apparently the correlation between Im M_{1-} and Im S_{1-} washes out the χ^2 minimum and increases the uncertainties in some of the parameters. Elimination of Im M_{1-} reduces the parameter uncertainties even though real $2-$ parameters are added to the basic *sp* fit. More importantly, elimination of Im M_{1-} improves the W dependencies of several of the multipoles, especially Im S_{1-}. Although the fitted value does not change appreciably and Im S_{1-} is not directly involved in the computation of SMR, its correlations with amplitudes that are needed for SMR are larger when Im M_{1-} is permitted to vary and tend to increase the uncertainty in SMR. Therefore, we consider the parameter space consisting of real $2-$ and all s- and p-wave amplitudes except Im M_{1-} to be optimal and describe it as the final fit.

TABLE I: Quadrupole ratios for $W = 1.23$ GeV at $Q^2 = 1.0$ (GeV/c)^2 using the pseudovector Born baseline model. Only statistical uncertainties from fitting are given.

variables	SMR, %	EMR, %	χ^2_ν
$0+, 1+, 1-$	-6.73 ± 0.24	-2.43 ± 0.19	1.69
$0+, 1+, 1-, 2-, 2+$	-6.95 ± 0.49	-3.19 ± 0.79	1.64
$0+, 1+, 1-, \mathrm{Re}\ 2-$	-6.85 ± 0.27	-2.73 ± 0.20	1.65
" except Im M_{1-}	-6.84 ± 0.15	-2.91 ± 0.19	1.65

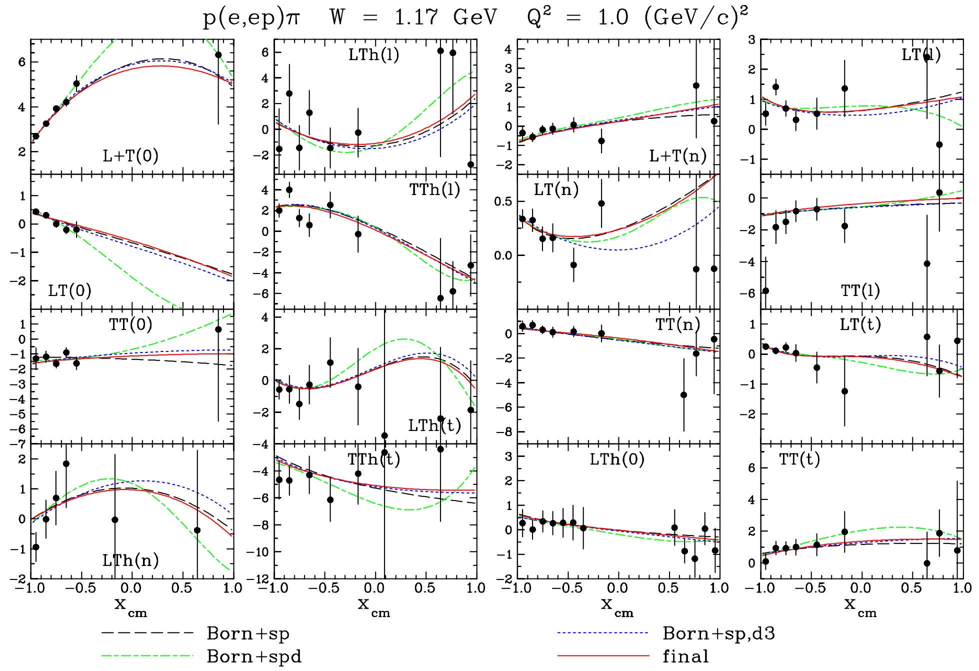

FIG. 15: Multipole fits for $W = 1.17$ GeV at $Q^2 = 1.0$ (GeV/c)^2 using a Born baseline model. Dashed curves fit corrections to all s- and p-wave amplitudes, blue dotted curves also fit real parts of $2-$ multipoles, and green dash-dotted curves fit all s-, p-, and d-wave amplitudes. The solid red curves, considered the final fit, are similar to the blue dotted curves except that Im M_{1-} is absent. See text for further details.

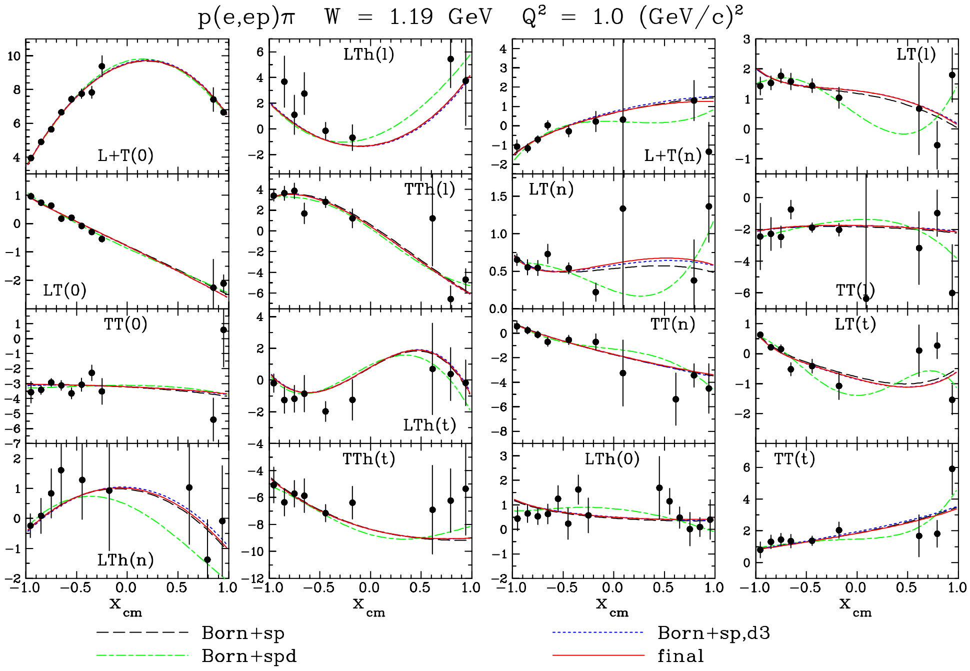

FIG. 16: Multipole fits for $W = 1.19$ GeV at $Q^2 = 1.0$ $(\text{GeV}/c)^2$ using a Born baseline model. See Fig. 15 for legend.

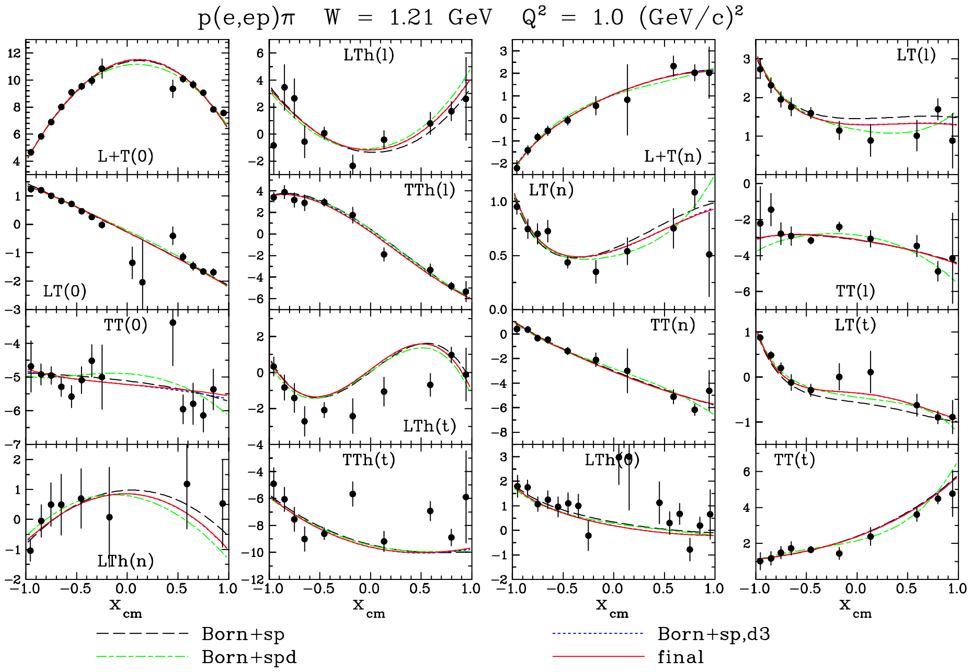

FIG. 17: Multipole fits for $W = 1.21$ GeV at $Q^2 = 1.0$ $(\text{GeV}/c)^2$ using a Born baseline model. See Fig. 15 for legend.

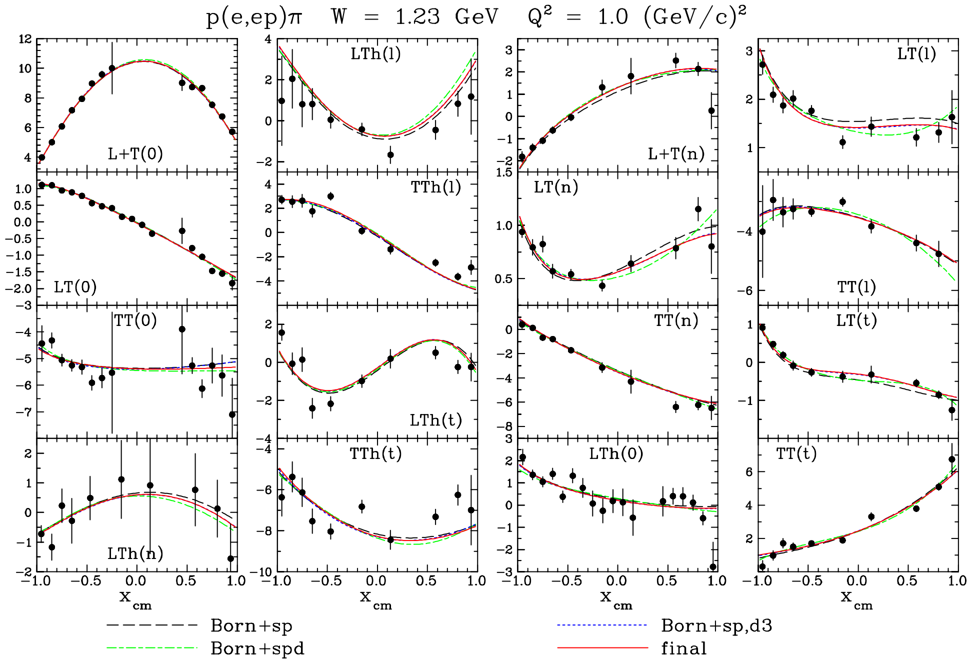

FIG. 18: Multipole fits for $W = 1.23$ GeV at $Q^2 = 1.0$ (GeV/c)^2 using a Born baseline model. See Fig. 15 for legend.

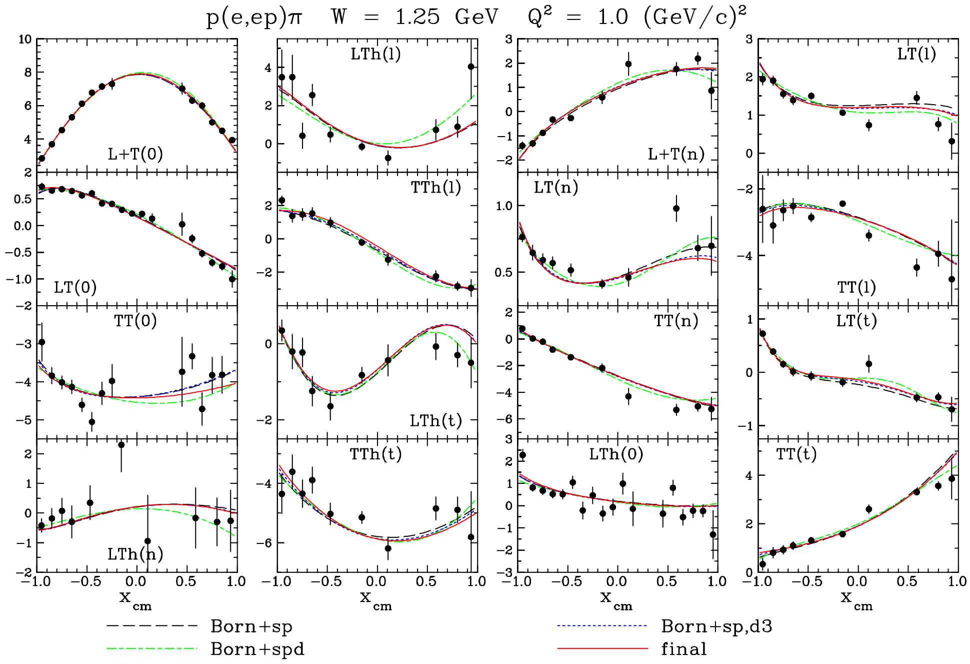

FIG. 19: Multipole fits for $W = 1.25$ GeV at $Q^2 = 1.0$ (GeV/c)^2 using a Born baseline model. See Fig. 15 for legend.

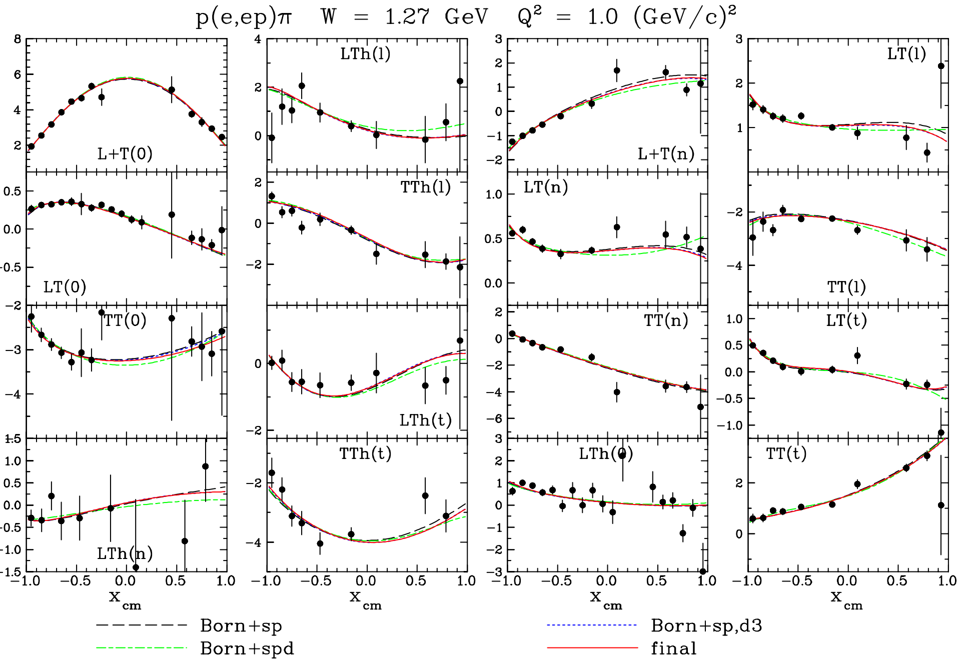

FIG. 20: Multipole fits for $W = 1.27$ GeV at $Q^2 = 1.0$ (GeV/c)^2 using a Born baseline model. See Fig. 15 for legend.

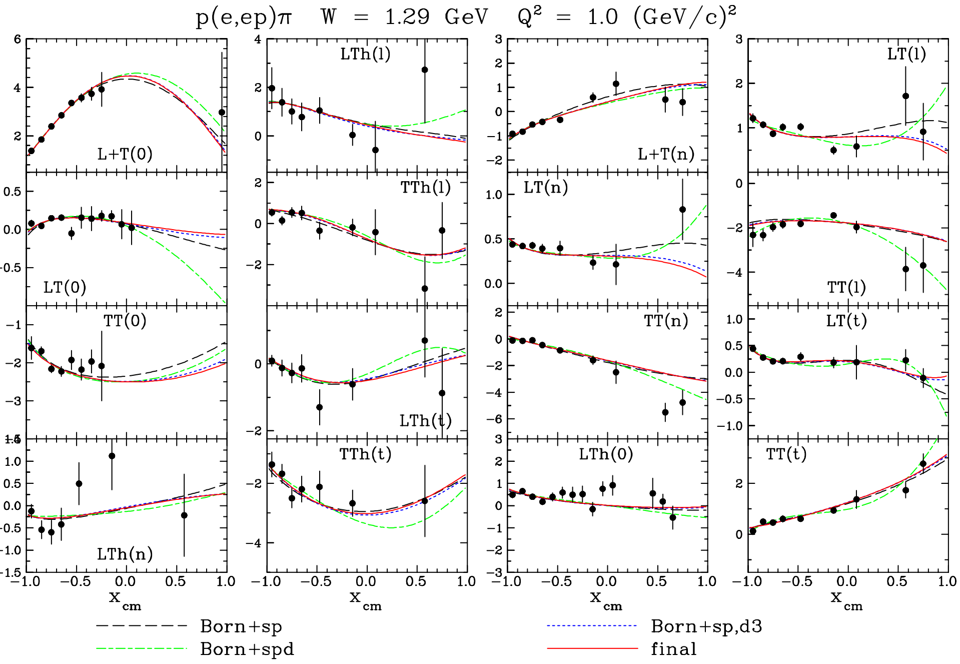

FIG. 21: Multipole fits for $W = 1.29$ GeV at $Q^2 = 1.0$ (GeV/c)^2 using a Born baseline model. See Fig. 15 for legend.

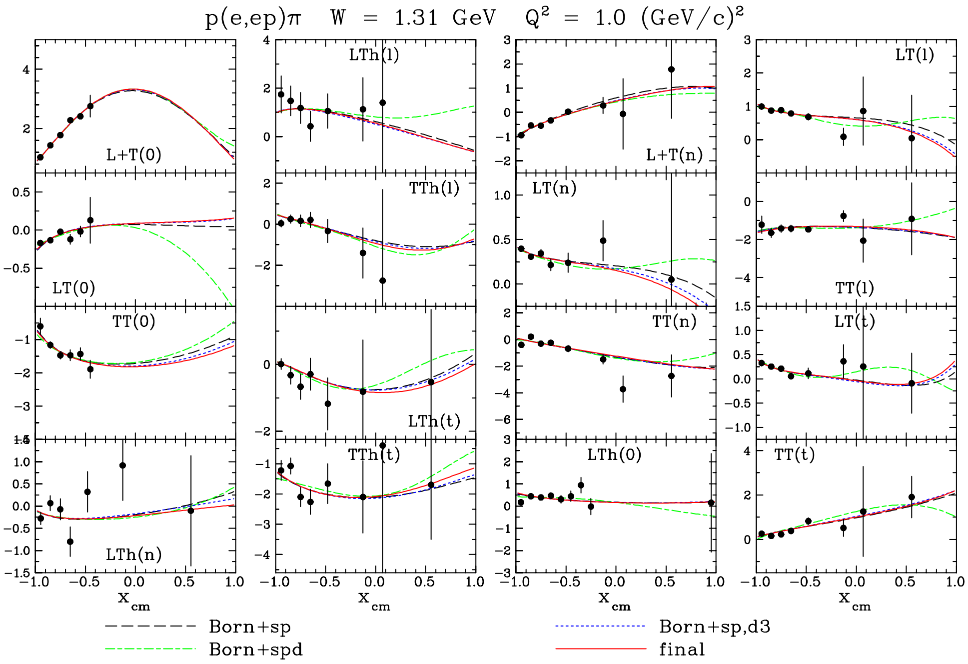

FIG. 22: Multipole fits for $W = 1.31$ GeV at $Q^2 = 1.0$ (GeV/c)^2 using a Born baseline model. See Fig. 15 for legend.

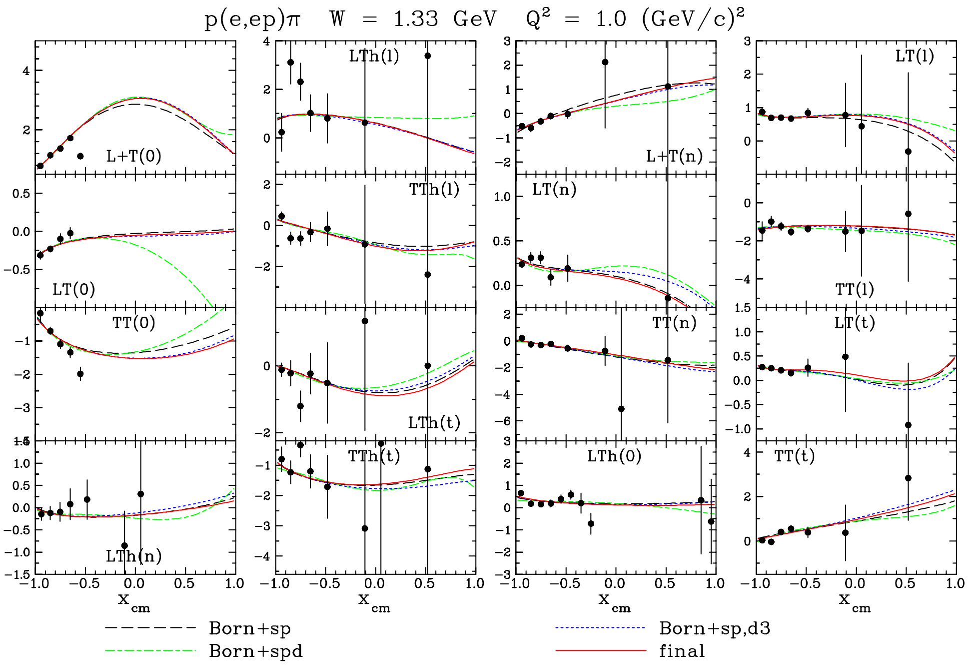

FIG. 23: Multipole fits for $W = 1.33$ GeV at $Q^2 = 1.0$ (GeV/c)^2 using a Born baseline model. See Fig. 15 for legend.

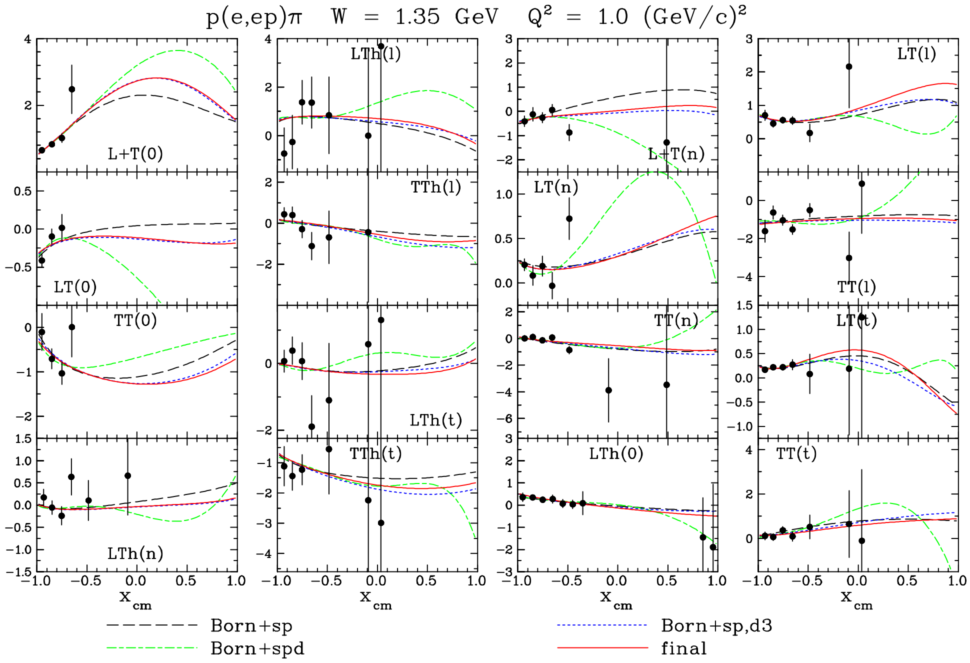

FIG. 24: Multipole fits for $W = 1.35$ GeV at $Q^2 = 1.0$ (GeV/c)^2 using a Born baseline model. See Fig. 15 for legend.

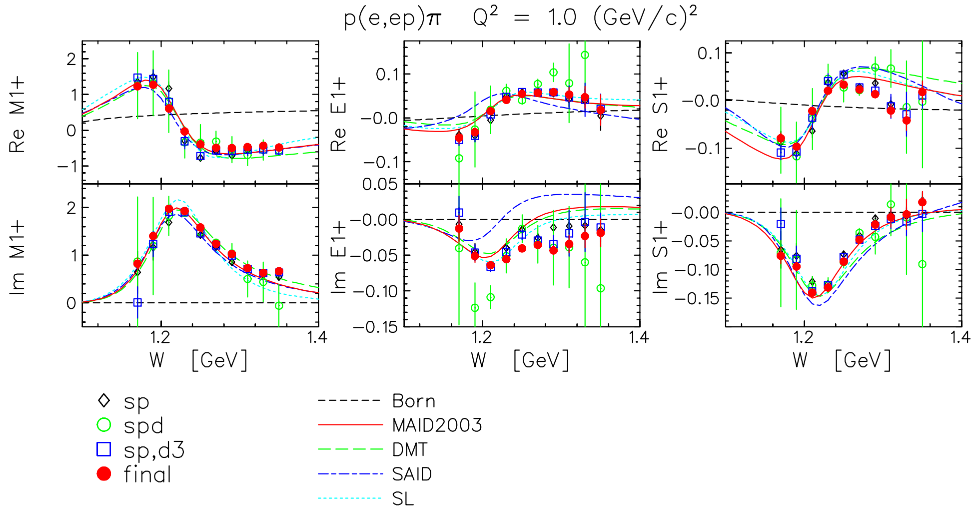

FIG. 25: Fitted multipole amplitudes using Born baseline. Black diamonds fit s- and p-waves, blue squares also fit real parts of 2− multipoles, and green open circles fit all $\ell \leq 2$ amplitudes. The final results, shown as red filled circles, are similar to the blue squares except that Im M_{1-} was constrained to zero. Several other recent models are shown also: MAID2003 (solid), DMT (short-dashed), SAID (long-dashed), and SL (dash-dotted).

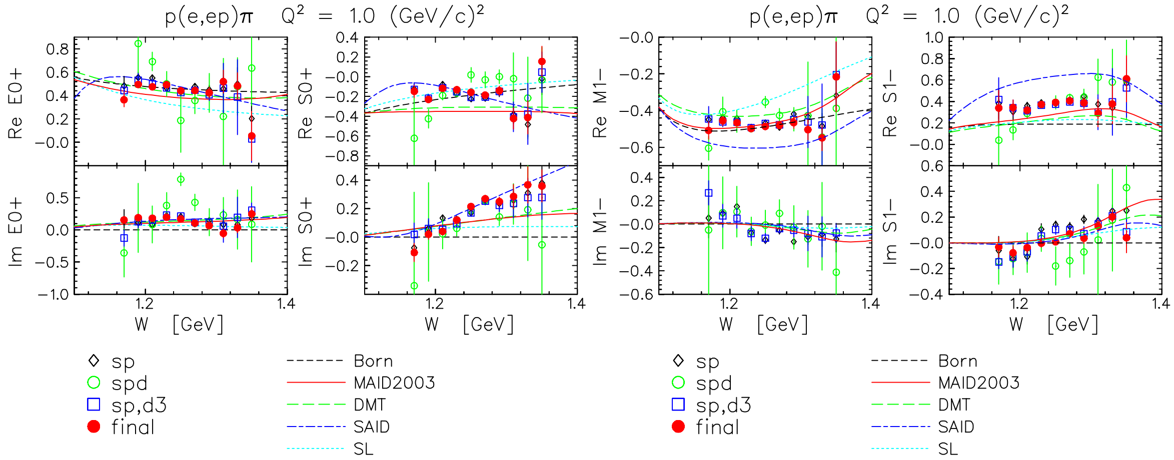

FIG. 26: Fitted multipole amplitudes using Born baseline. See Fig. 25 for legend.

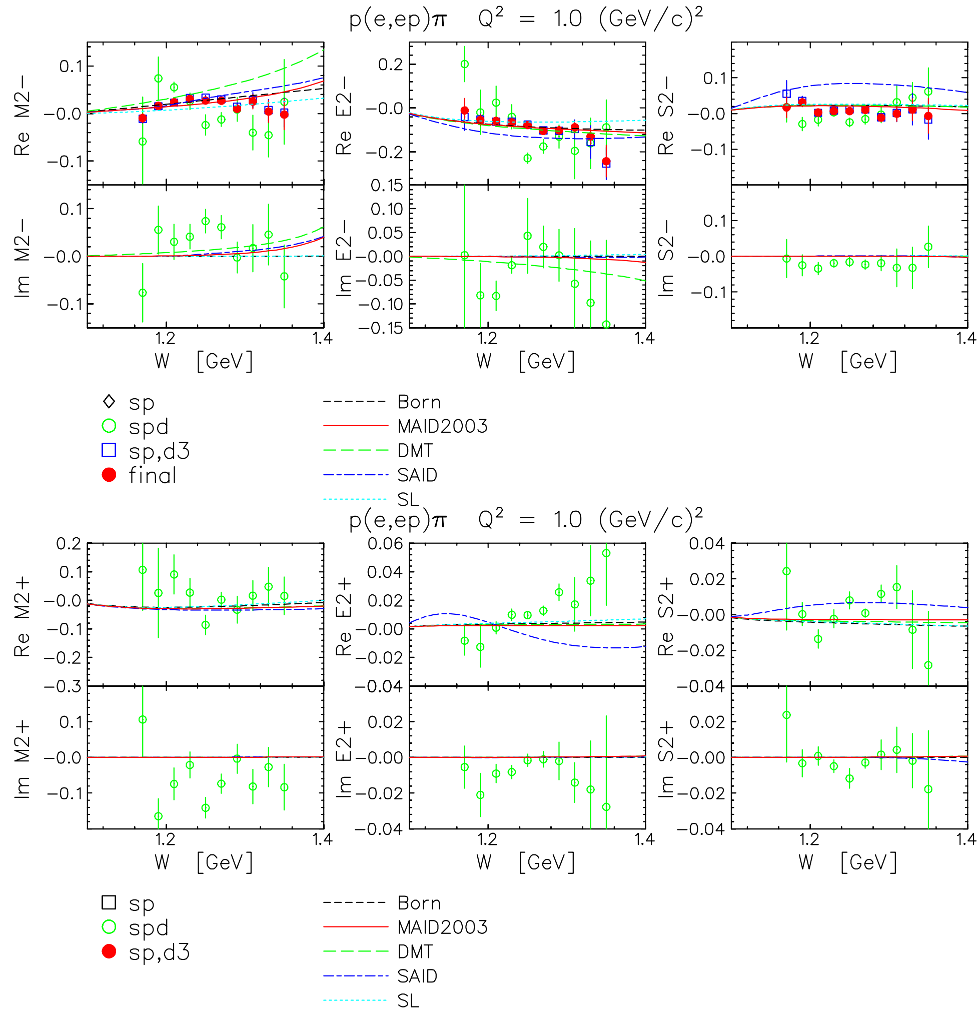

FIG. 27: Fitted multipole amplitudes using Born baseline. See Fig. 25 for legend.

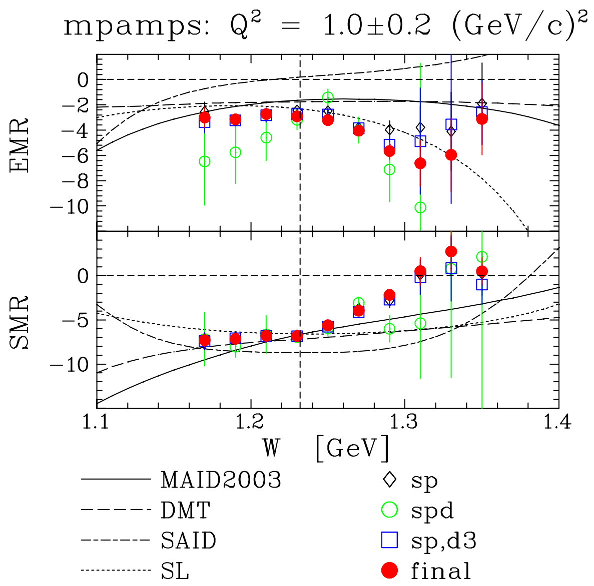

FIG. 28: Sensitivity of fitted quadrupole ratios to the number of adjustable amplitudes. See Fig. 25 for legend.

TABLE II: Dependence of quadrupole ratios for $W = 1.23$ GeV at $Q^2 = 1.0$ $(\mathrm{GeV}/c)^2$ upon baseline model. All s- and p-wave amplitudes except Im M_{1-} plus real $2-$ amplitudes were fit with other amplitudes given by the specified baseline model.

baseline	SMR, %	EMR, %	χ^2_ν
Born	-6.84 ± 0.15	-2.91 ± 0.19	1.65
MAID2003	-6.90 ± 0.15	-2.79 ± 0.19	1.67
DMT	-6.82 ± 0.15	-2.70 ± 0.19	1.67
SL	-6.79 ± 0.15	-2.81 ± 0.19	1.64
SAID	-7.38 ± 0.15	-2.53 ± 0.20	1.85

IV. SENSITIVITY TO BASELINE MODEL

The insensitivity of the multipole analysis to the choice of baseline model is illustrated by Figs. 29-38 for response functions and Figs. 39-41 for multipole amplitudes. These fits vary all s- and p-wave multiples, except Im M_{1-}, plus real parts of $2-$ multipoles; all other multipoles are determined by the specified baseline model. The fits based upon Born, MAID2003, DMT, or SL models are practically indistinguishable. The fits based upon SAID display a more oscillatory structure that is not supported by the data in the middle of the W range where the precision is best. The oscillations are presumably due to relatively large Re E_{2+} and Re S_{2+} amplitudes that are not ameliorated by the current truncation scheme. Therefore, the data clearly require smaller $2+$ amplitudes than predicted by the SAID model.

Similarly, the fitted multipole amplitudes are rather insensitive to the choice of baseline model. Even the fits based upon SAID, starting from rather different initial conditions and with significantly larger fixed $2+$ amplitudes, converge upon essentially the same final results. Therefore, the fitted amplitudes are practically model independent.

Figure 42 shows the sensitivity of fitted quadrupole ratios to the choice of baseline model. The curves show quadrupole ratios for the various models while points show ratios fit to data using the corresponding baseline model for the partial waves that were not permitted to vary. EMR shows a little more sensitivity than SMR to the choice of baseline model, but variations near the Δ pole position remain within about one standard deviation. The largest discrepancy for EMR is seen with the SAID baseline model and is probably caused by its relatively large $2+$ multipoles. Nevertheless, the fitted quadrupole ratios show very little sensitivity to the baseline model, especially in the crucial region around the Δ pole position. Therefore, it is clear that the data determine EMR and SMR with rather little dependence upon the model for background partial waves.

Note that Fig. 42 also shows quadrupole ratios for the Born baseline model, but that those curves must be interpreted with care. The Born multipole amplitudes are real while the $1+$ amplitudes for more complete models are close to pure imaginary near the Δ pole. Although the small real $1+$ Born amplitudes give quadrupole ratios with magnitudes similar to those for models with resonances, their origin is quite different; EMR even has the opposite sign near $W = 1.23$ GeV.

Finally, Table II lists the quadrupole ratios for $W = 1.23$ GeV based upon several choices of baseline models and using the "final" parameter space. All of the results are consistent except those using the SAID baseline, for which SMR is substantially higher and EMR lower than for other baseline models. However, the quality of the fit is also noticeably inferior even though the differences in $\chi^2_n u$ are not impressive. Therefore, we conclude that this version of the SAID model does not provide a suitable baseline for multipole analysis and judge the sensitivity to uncertainties in the baseline model to be similar to the tabulated fitting uncertainties.

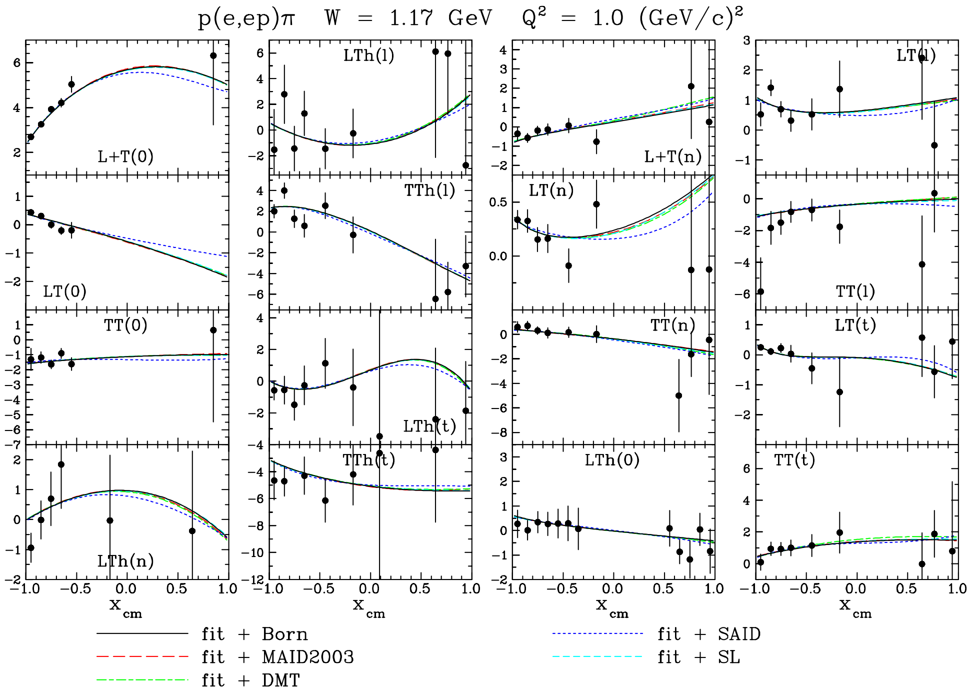

FIG. 29: Sensitivity of multipole fits for $W = 1.17$ GeV at $Q^2 = 1.0$ $(\mathrm{GeV}/c)^2$ to the choice of baseline model. Black solid, red dashed, green dash-dotted, blue dotted, and cyan short-dashed curves are based upon Born, MAID2003, DMT, SAID, and SL models, respectively. See text for details.

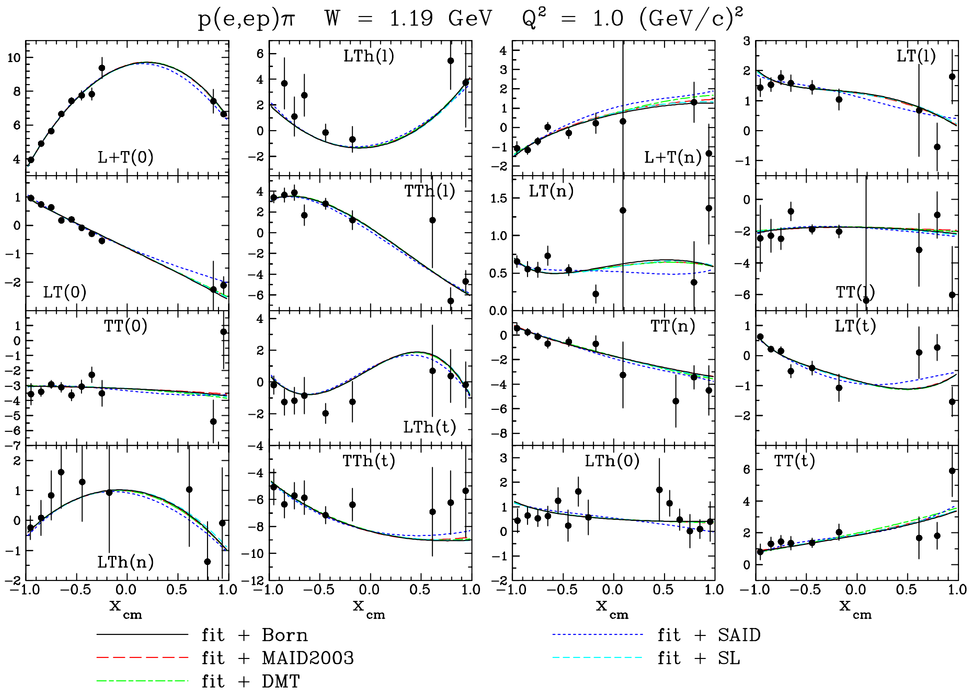

FIG. 30: Sensitivity of multipole fits for $W = 1.19$ GeV at $Q^2 = 1.0$ $(\mathrm{GeV}/c)^2$ to the choice of baseline model. See Fig. 29 for legend.

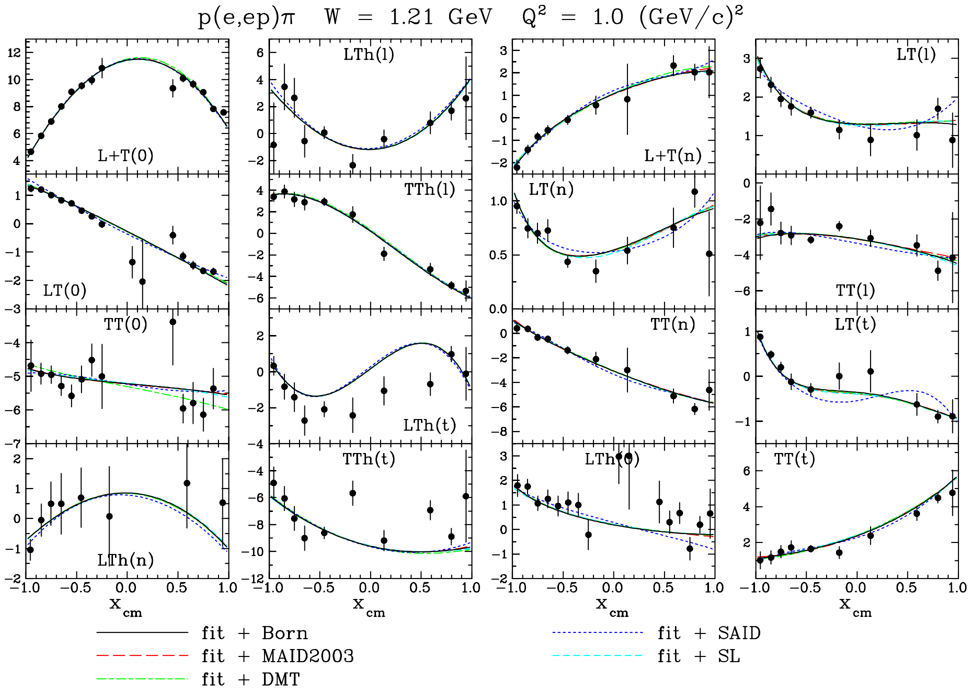

FIG. 31: Sensitivity of multipole fits for $W = 1.21$ GeV at $Q^2 = 1.0$ $(\mathrm{GeV}/c)^2$ to the choice of baseline model. See Fig. 29 for legend.

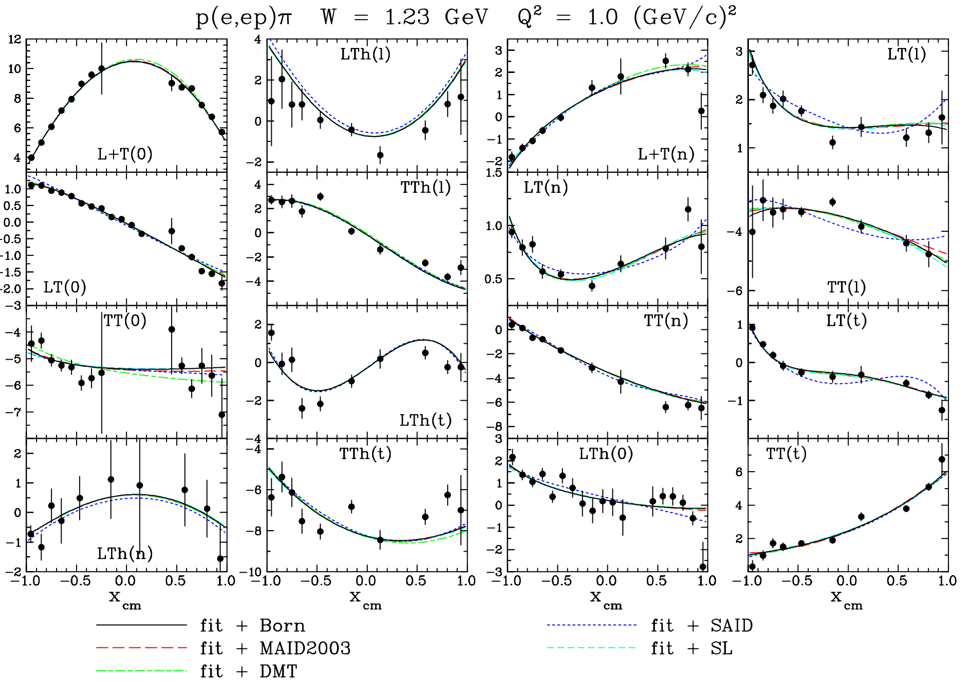

FIG. 32: Sensitivity of multipole fits for $W = 1.23$ GeV at $Q^2 = 1.0$ $(\mathrm{GeV}/c)^2$ to the choice of baseline model. See Fig. 29 for legend.

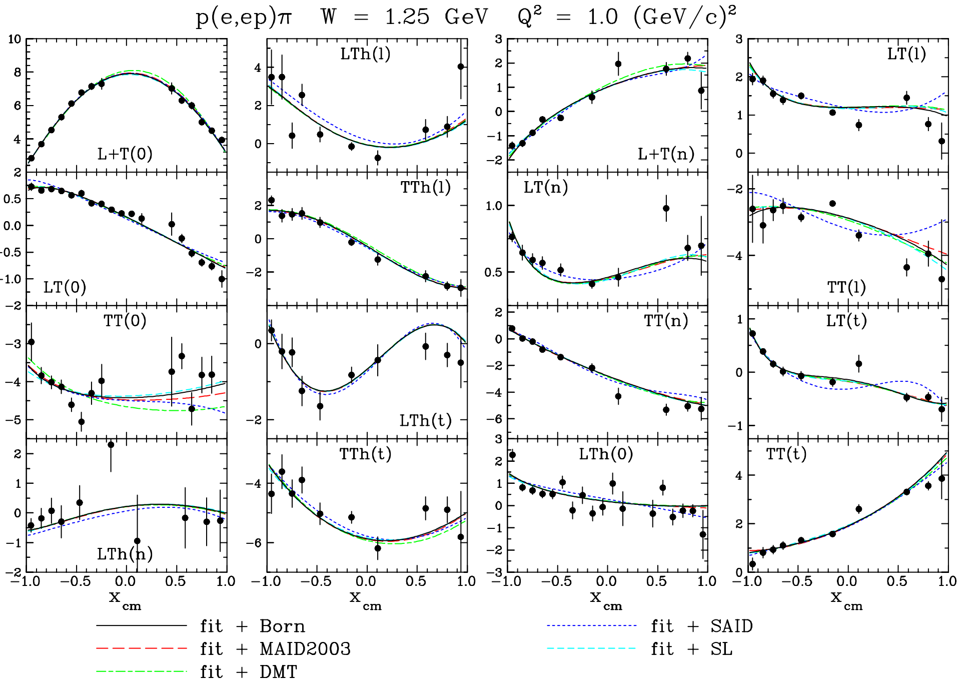

FIG. 33: Sensitivity of multipole fits for $W = 1.25$ GeV at $Q^2 = 1.0$ (GeV/c)^2 to the choice of baseline model. See Fig. 29 for legend.

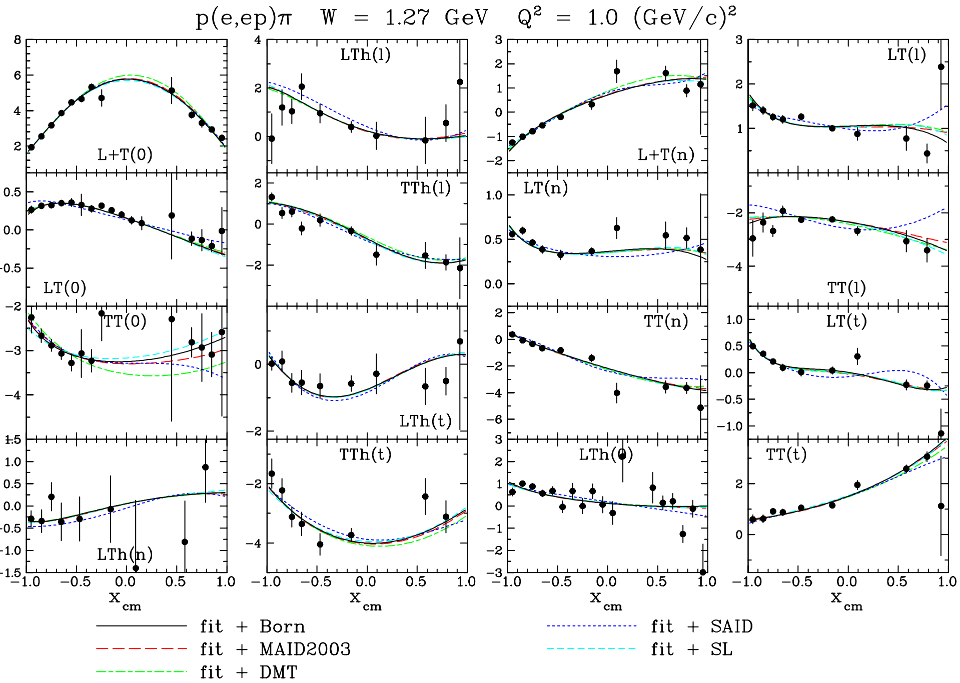

FIG. 34: Sensitivity of multipole fits for $W = 1.27$ GeV at $Q^2 = 1.0$ (GeV/c)^2 to the choice of baseline model. See Fig. 29 for legend.

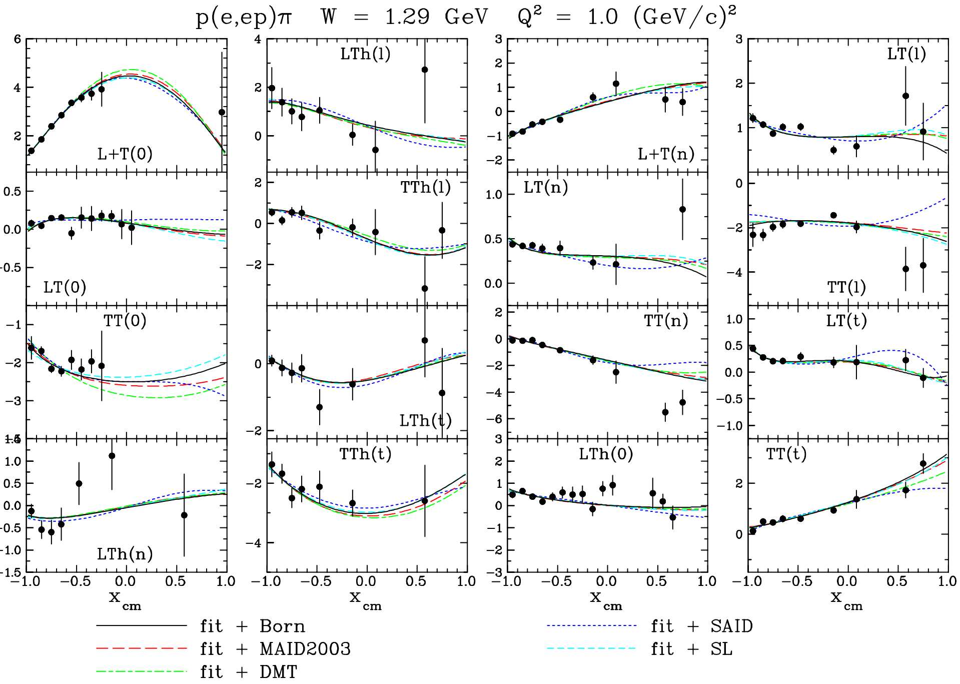

FIG. 35: Sensitivity of multipole fits for $W = 1.29$ GeV at $Q^2 = 1.0$ (GeV/c)^2 to the choice of baseline model. See Fig. 29 for legend.

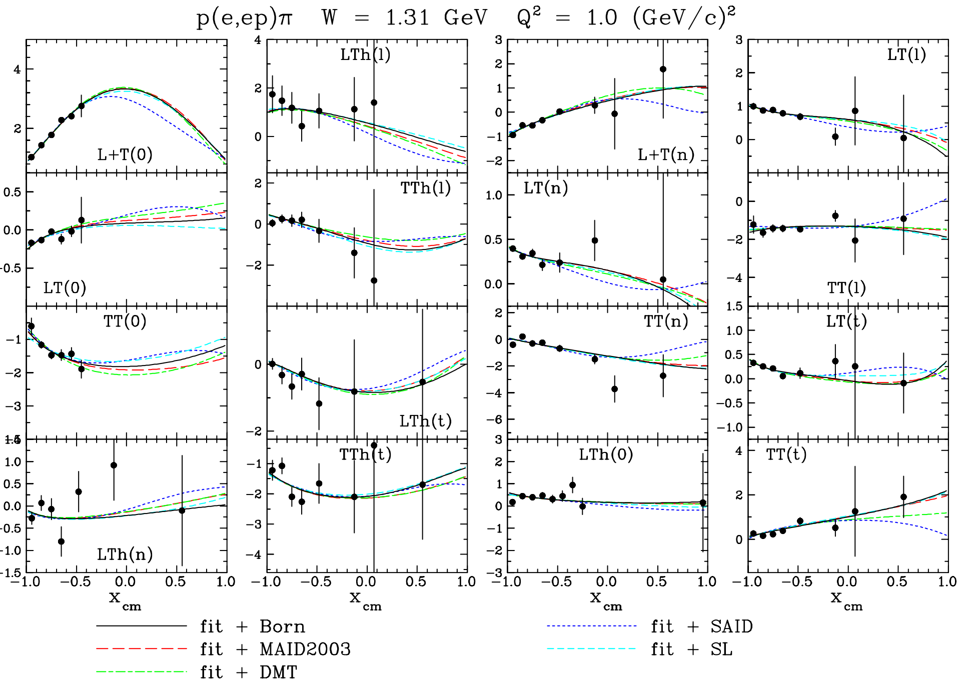

FIG. 36: Sensitivity of multipole fits for $W = 1.31$ GeV at $Q^2 = 1.0$ (GeV/c)^2 to the choice of baseline model. See Fig. 29 for legend.

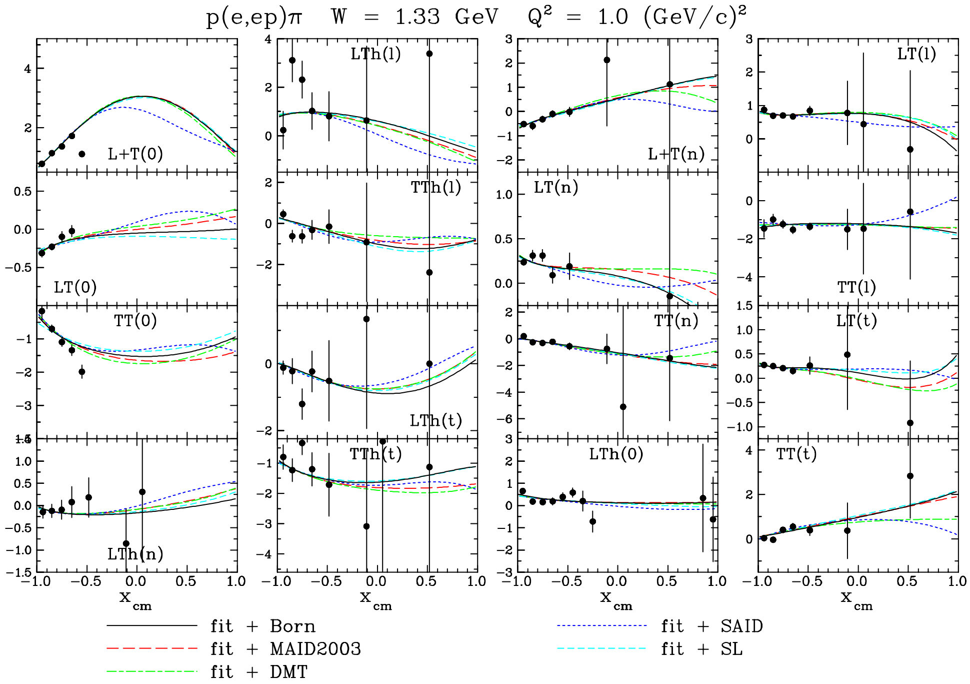

FIG. 37: Sensitivity of multipole fits for $W = 1.33$ GeV at $Q^2 = 1.0$ (GeV/c)^2 to the choice of baseline model. See Fig. 29 for legend.

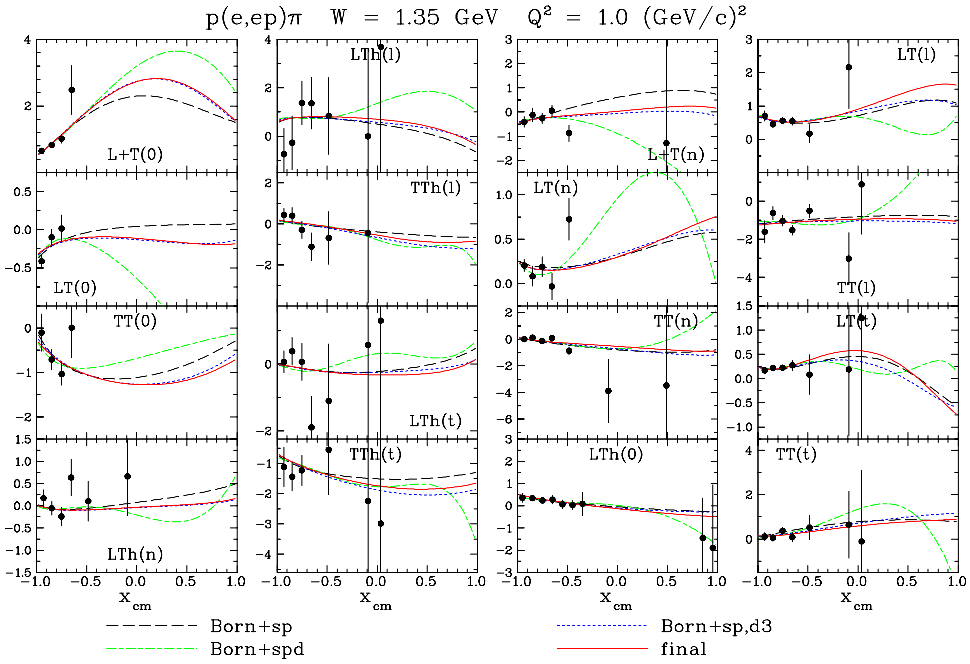

FIG. 38: Sensitivity of multipole fits for $W = 1.35$ GeV at $Q^2 = 1.0$ (GeV/c)^2 to the choice of baseline model. See Fig. 29 for legend.

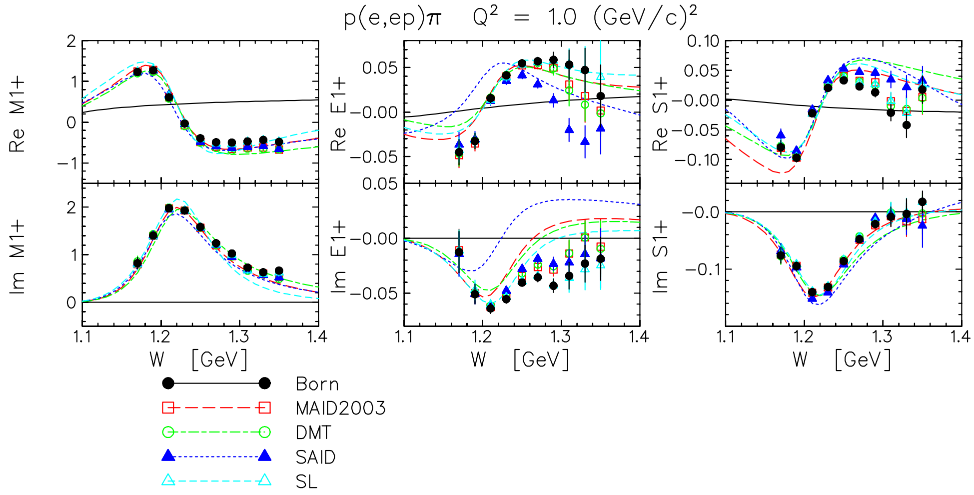

FIG. 39: Sensitivity of fitted multipole amplitudes to the choice of baseline model. Black filled circles and solid curves are based upon Born, red squares and dashed curves upon MAID2003, green open circles and dash-dotted curves upon DMT, blue filled triangles and dotted curves upon SAID, and cyan open triangles and short-dashed curves upon SL baseline models, respectively. See text for details.

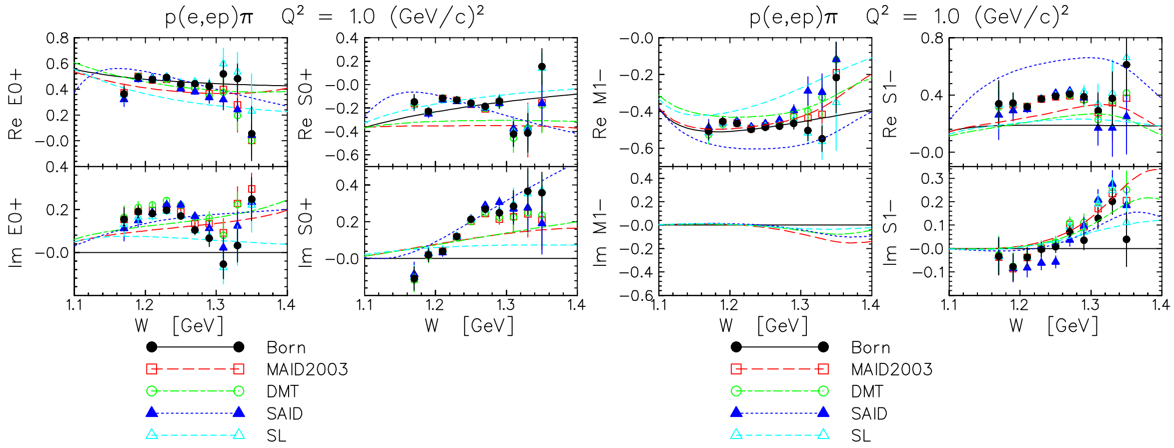

FIG. 40: Sensitivity of fitted multipole amplitudes to the choice of baseline model. See Fig. 39 for legend.

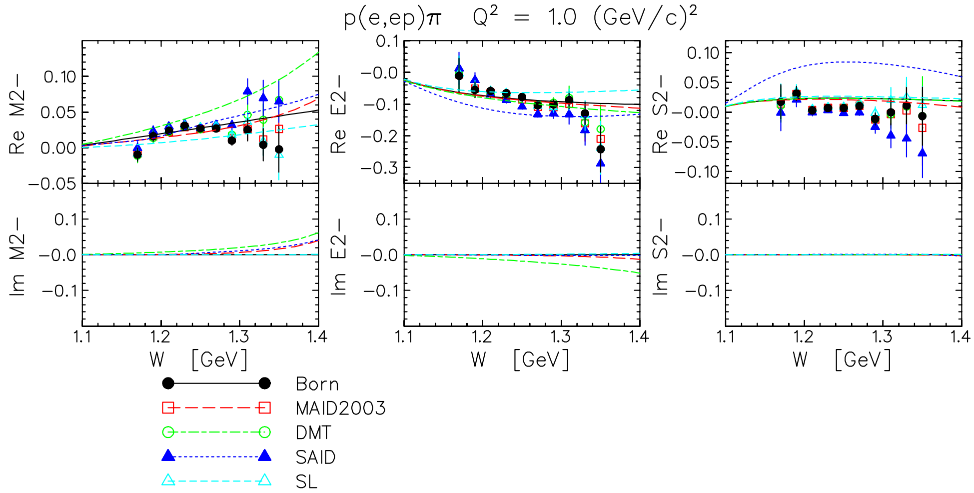

FIG. 41: Sensitivity of fitted multipole amplitudes to the choice of baseline model. See Fig. 39 for legend.

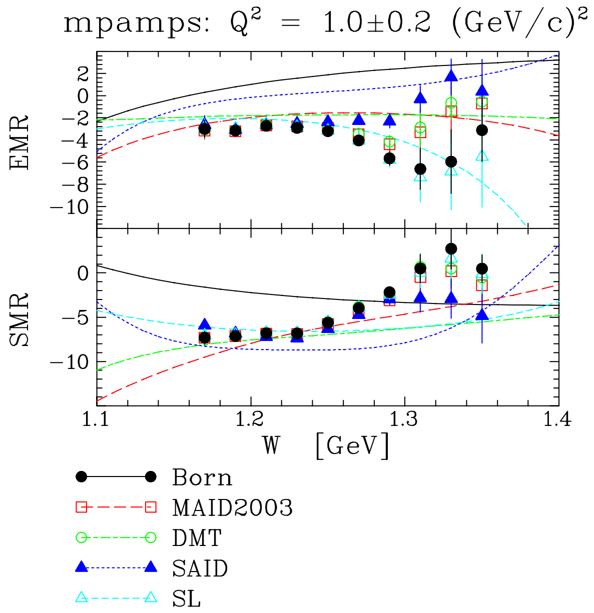

FIG. 42: Sensitivity of fitted quadrupole ratios to the choice of baseline model. See Fig. 39 for legend.

V. SYSTEMATIC UNCERTAINTIES

Although there are too many calibration parameters and the propagation of errors is far too complicated to perform a truly rigorous analysis of systematic errors for either the response-function data or the fitted multipole amplitudes, we expect those uncertainties to be generally smaller than the statistical uncertainties. Therefore, we believe that it is sufficient to perform a more schematic analysis of some of the dominant systematic uncertainties. Our basic strategy is to evaluate the sensitivity of extracted quantities to small variations of various parameters sequentially and to add numerical derivatives of fitted quantities in quadrature. For example, the systematic uncertainty due to FPP analyzing power is estimated by applying a common scale factor to all recoil-polarization data, fitting the scaled data, and comparing the fitted multipole parameters to those obtained with nominal scale factors. We do not consider separate variations for each analyzer thickness or momentum setting, which would require many replays. Similarly, we assume that the beam polarization has a common systematic scale uncertainty that affects all helicity-dependent polarization and response data and that there is a common normalization uncertainty for cross sections and response functions.

Let $y(\lambda_i)$ represent a quantity, such as a quadrupole ratio or multipole amplitude, fitted to a data set for which one of the scale factors has the value λ_i. The net systematic error then takes the form

$$(\delta y)^2_{\rm sys} = \sum_i \left(\frac{\partial y}{\partial \lambda_i} \delta\lambda_i \right)^2 = \sum_i \left(y(\lambda_i + \delta\lambda_i) - y(\lambda_i) \right)^2 \tag{2}$$

where most scale factors would have nominal values of $\lambda_i = 1$. Dependencies on fixed parameters are suppressed. The following systematic effects will be considered. Further details can be found in Ref. [8].

normalization: a common normalization uncertainty for differential cross sections and response functions estimated at $\pm 3\%$.

beam polarization: the systematic relative uncertainty for Compton measurements of beam polarization is estimated to be about 1.4% [9].

analyzing power: the relative uncertainties in average analyzing power reported by Punjabi *et al.* [10] are in the $1-2\%$ range. Because we do not consider thickness or momentum variations, we adopt a fairly conservative estimate of $\delta A_y / A_y = 0.02$.

elastic subtraction: the correction for elastic contamination is small and only affects bins with $x_{cm} = -0.15$ and 0.2, but the contamination fractions binned in ϕ were difficult to determine. Therefore, we estimated the systematic uncertainty due to elastic contamination using a relative uncertainty of 100% in its scale factor. The effect on fitted multipole amplitudes and quadrupole ratios remains negligible despite this generous uncertainty.

false asymmetry: the systematic uncertainty due to the corrections for false asymmetry are estimated by comparing fits to data replayed with and without false asymmetry. We assume that the relative uncertainty in false asymmetry is approximately 10%.

spin rotation: the systematic uncertainties due to spin rotation are analyzed using a simplified parametrization based upon two trajectory angles and four matrix elements coupling spin and trajectory angles [10, 11]. Uncertainties due to each of these parameters are evaluated by comparing replays with modified and nominal values for those angles. We use the same uncertainties in the spin rotation parameters and angle reconstructions that were reported in Refs. [10, 11].

bin centering: variations of the acceptance-averaged Q^2 with x_{cm} are compensated in multipole fits using a model form factor. Therefore, we evaluate the sensitivity of fitted quantities to uncertainties in the appropriate form factor by comparing results using the Sato-Lee $N \to \Delta$ form factor [7] with those for the standard dipole form factor.

Sensitivity to variations of each of the 6 Pentchev spin rotation parameters [10, 11] was evaluated by comparing replays performed with a perturbation of that parameter with the replay using nominal values of those parameters. Each fit was started from the same initial conditions, corresponding to the results of the nominal Pentchev analysis. Similarly, sensitivities to all other parameters were evaluated by comparison with the final fit from Sec. III starting from those parameters. As discussed in Ref. [8] this procedure is intended to estimate small shifts of a particular minimum due to small distortions of the χ^2 hypersurface by each parameter variation. The 12 systematic uncertainties described above were then added in quadrature and combined with the statistical uncertainties for the final fit to

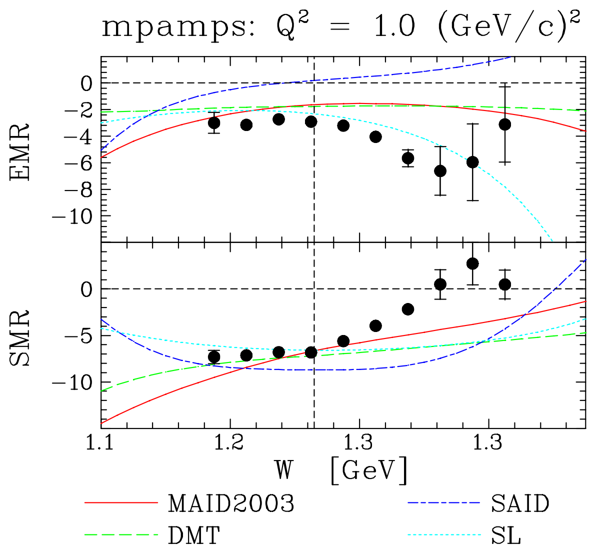

FIG. 43: Quadrupole amplitudes with statistical uncertainties shown as inner error bars with endcaps and systematic uncertainties as outer error bars without endcaps. Red solid curves show MAID2003, green dashed DMT, blue dash-dotted SAID, and cyan dotted SL calculations.

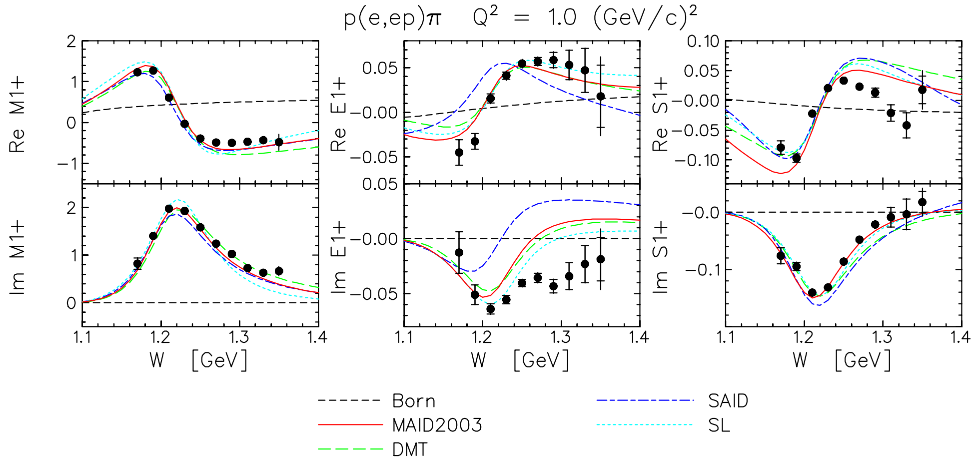

FIG. 44: Multipole amplitudes with statistical uncertainties shown as inner error bars with endcaps and systematic uncertainties as outer error bars without endcaps. See Fig. 43 for legend.

obtain total uncertainties in each of the fitted multipole parameters. This analysis is based upon the pseudovector Born baseline model and use the "final" selection of variable parameters chosen Sec. III, including all s- and p-wave amplitudes except Im M_{1-} plus real parts of $2-$ amplitudes.

The systematic uncertainties in quadrupole ratios and multipole amplitudes are illustrated in Figs. 43-46. Inner error bars show statistical uncertainties while outer error bars add systematic uncertainties in quadrature. Systematic uncertainties are generally smaller than statistical uncertainties and usually difficult to discern. Their contributions to the quadrupole ratios are negligible near the pole position.

VI. DISCUSSION

A. Multipole amplitudes

We have found that the sensitivities of fitted multipole amplitudes to the truncation scheme or the choice of baseline model are small and that uncertainties due to systematic errors in response functions are generally smaller than statistical or fitting uncertainties. Therefore, the fitted multipole amplitudes can be described as nearly model

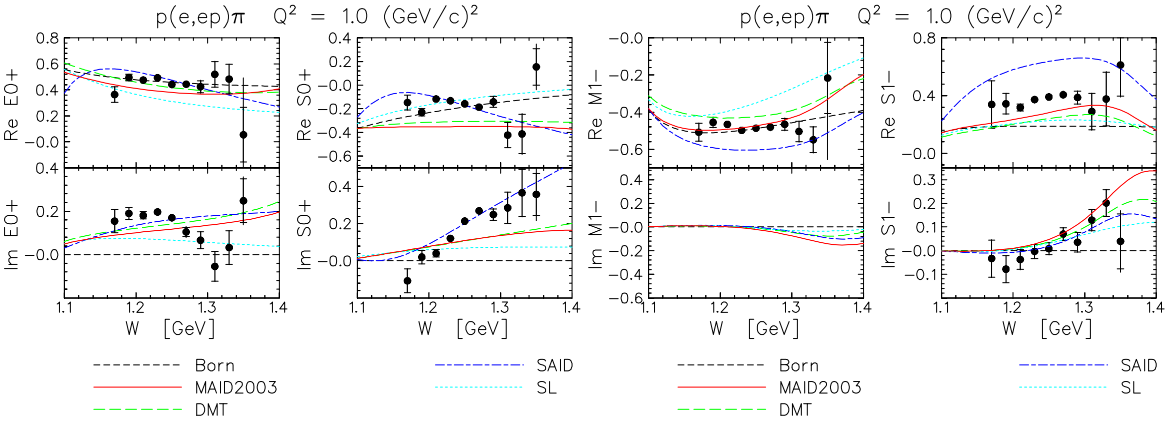

FIG. 45: Multipole amplitudes with statistical uncertainties shown as inner error bars with endcaps and systematic uncertainties as outer error bars without endcaps. See Fig. 43 for legend.

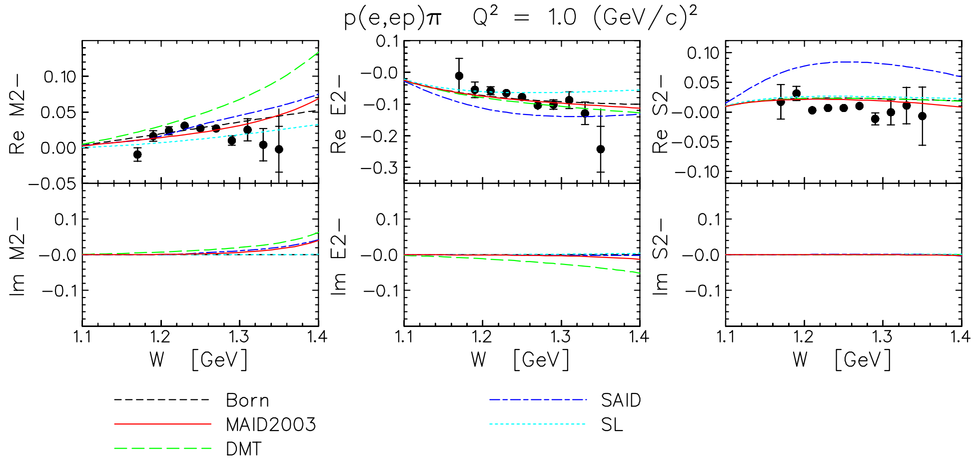

FIG. 46: Multipole amplitudes with statistical uncertainties shown as inner error bars with endcaps and systematic uncertainties as outer error bars without endcaps. See Fig. 43 for legend.

independent.

There is rather little spread among models for M_{1+} amplitudes across the $\Delta(1232)$ resonance and our experimental amplitudes agree well with model calculations even when the fit is based upon a Born baseline model without resonances. The variation among models is also relatively small for S_{1+} amplitudes and good agreement is obtained with data for Im S_{1+}, but for the real part the present data exhibit a steeper slope on the large W side. MAID2003, DMT, and SL calculations are similar for E_{1+}, but the current SAID calculations are substantially different and disagree with the data. Our results for Re E_{1+} agree relatively well with MAID2003, DMT, or SL but the Im E_{1+} data do not show the node near $W \approx 1.27$ GeV predicted by those models; there is no sign change for $W \leq 1.35$ GeV.

Among the models considered, MAID2003 tends to provide the best description of the recoil-polarization data, but it does not reproduce the R^{ℓ}_{LT}, R^{t}_{LT}, or R^{n}_{LT} angular distributions particularly well. These difficulties appear to arise primarily from the S_{0+} amplitudes. Whereas MAID2003 suggests a nearly constant Re S_{0+} amplitude in this W range, we find less negative results with a significant negative slope in W. Although the SL calculation crosses the Re S_{0+} data near the middle of the W range, it has the opposite slope. We also find a rather steep slope for Im S_{0+}. It is interesting to observe that the SAID model agrees best with the 0+ amplitudes even though it is worst, among these models, for E_{1+}, Re 1−, and S_{2-}. All of the models agree pretty well with the Re E_{0+} data, but none reproduce the W dependence seen for Im E_{0+}.

It is also interesting to observe that there is a wide spread among the models for Re M_{1-} but that the data are closest to the Born model that omits the Roper resonance, suggesting that ${}_pA_{1/2}$ is small. Note that the analysis of CLAS data for $Q^2 = 0.4$ and 0.65 $(\mathrm{GeV}/c)^2$ by Aznauryan *et al.* [12] suggests a rapid slope for ${}_pA_{1/2}(Q^2)$ with a sign change between 0.4 and 0.65 $(\mathrm{GeV}/c)^2$. In Ref. [1] we present an independent fit to the multipole amplitudes using the unitary isobar model and conclude that there is a substantial longitudinal contribution to S_{1-} attributable to the

TABLE III: Quadrupole ratios for $W = 1.23$ GeV at $Q^2 = 1.0$ (GeV/c)^2.

model	SMR, %	EMR, %	comment
final multipole analysis	-6.84 ± 0.15	-2.91 ± 0.19	Born baseline
Legendre Fit C	-6.11 ± 0.11	-1.92 ± 0.14	Ref. [14]
Joo *et al.* [13]	-7.4 ± 0.4	-1.8 ± 0.4	Weighted average for $Q^2 = 0.9$ (GeV/c)^2
MAID2003	-6.73	-1.65	
DMT	-7.21	-1.77	
SL	-6.59	-2.29	
SAID	-8.71	$+0.17$	

Roper resonance with a value of ${}_pS_{1/2}$ similar to that obtained by Aznauryan *et al.* [12]. However, there is little room in M_{1-} for transverse Roper excitation when we use pseudovector πNN coupling, which is favored by our results for $0+$ amplitudes. The fact that Aznauryan obtains a nonnegligible Roper ${}_pA_{1/2}$ is apparently due to the use of mixed PS/PV coupling, as prescribed by the MAID model. See Ref. [1] for further details.

The real $2-$ amplitudes are small in this W range, but the slope for Re E_{2-} appears to be determined well by these data and is in good agreement with Born, MAID2003, or DMT predictions. However, the predictions of the SAID model are much larger than the data for Re S_{2-}. SAID also predicts significant oscillations in $2+$ amplitudes that are absent in other models. Although we cannot fit the $2+$ amplitudes accurately, the large $\ell = 2$ amplitudes for SAID produce oscillations in many of the response functions that are not warranted by the data.

B. Quadrupole ratios

Table III compares the final fitted quadrupole ratios with model calculations, the CLAS results [13], and with a traditional Legendre analysis of our data [14]. The CLAS results should be compared with our Legendre analysis because both use similar methods. Thus, our Legendre EMR result is consistent with CLAS, but their SMR is substantially larger. On the other hand, our multipole analysis gives significantly larger quadrupole ratios, both transverse and longitudinal, than does our Legendre analysis of the same data. Recognizing that the traditional Legendre analysis is based upon sp truncation and M_{1+} dominance while the multipole analysis avoids those assumptions, we conclude that those approximations are not adequate given the statistical precision of the Hall A data. The sensitivity of the traditional Legendre analysis to truncation errors is studied in more detail in Ref. [15]. The fact that the CLAS error bar overlaps the SMR result from our multipole analysis is considered an accident arising from the disagreement between the two Legendre analyses for SMR; the Legendre method is not sufficiently accurate for our purposes. Our SMR result is similar to those predicted by MAID2003, DMT, or SL, but is substantially smaller than the SAID prediction. Our EMR result is significantly stronger than the MAID2003, DMT, or SL predictions. This is consistent with the observation that Im E_{1+} is stronger than predicted by those models and remains negative throughout this range of W. SAID, on the other hand, has an earlier node in Im E_{1+} and thus predicts a small EMR with sign opposite that of other models and the present experimental result.

It is also of interest to parametrize the energy dependence of the quadrupole ratios, which facilitates interpolation to a nominal value for M_Δ. The W dependencies of multipole analyses for EMR and SMR are fit in Fig. 47 with parabolas of the form

$$y = \sum_{k=0}^{2} a_k (W - M_\Delta)^k \tag{3}$$

using a nominal value of $M_\Delta = 1.232$ GeV. The fits were confined to the central region, indicated by dotted vertical lines, where this simple parametrization should suffice for interpolation. Both fits describe the data for the central region well. The expansion coefficients are given in Table IV, where the data for quadrupole ratios are expressed in percent and where the multipole amplitudes are based upon the Born baseline. The a_0 parameters represent the best estimates of the quadrupole ratios at M_Δ but weighted linear least-squares fits with only 2 degrees of freedom do not necessarily provide realistic uncertainties. Instead, we quote the largest of $\delta R(1.23)$, δa_0, and $\delta a_0 \sqrt{\chi^2_\nu}$ where $\delta R(1.23)$ is the uncertainty in the single-energy fit to data for $W = 1.23$ GeV, δa_0 is the uncertainty in the value of a_0 according to the linear least-squares fit to the energy dependence, and χ^2_ν is the reduced chisquare for that fit in the central region. The second-order terms are negligible between M_Δ and the nearest W bin and changes due to the linear terms are less than one standard deviation. For example, the fitted EMR and SMR values for the multipole analysis are -2.85 and -6.69% at $W = 1.23$ GeV. The remaining differences between these values and those listed on

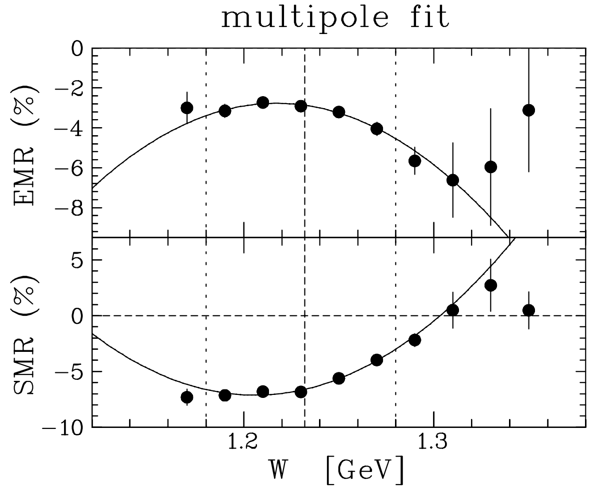

FIG. 47: Parabolic fits to the W dependence of quadrupole ratios from the multipole analyses based upon the Born baseline. Vertical dashed and dotted lines show M_Δ and the fitted ranges of W.

TABLE IV: Power series for quadrupole ratios in terms of $(W - M_\Delta)$ in units of GeV.

EMR				SMR			
a_0	a_1	a_2	χ^2_ν	a_0	a_1	a_2	χ^2_ν
-2.87 ± 0.19	-13.3	-450	0.15	-6.61 ± 0.18	39.3	749	2.16

the last line of Table I are less than one standard deviation. Therefore, although the quadrupole ratios in Table IV are slightly smaller than those reported in Ref. [16] using the same data, the results are consistent — the differences are partly due to variations with respect to W and partly due to statistical fluctuations of the data for 1.23 GeV relative to the average trends represented by the curves in Fig. 47.

VII. SUMMARY

We have performed a multipole analysis of $p(\vec{e}, e'\vec{p})\pi^0$ data at $Q^2 = 1$ (GeV/c)^2 for $1.17 \leq W \leq 1.35$ GeV in 10 bins of W across the $\Delta(1232)$ resonance. The data consist of differential cross section, beam analyzing power, and recoil-polarization response functions. We used pseudodata to test two methods for compensating the x-dependence of acceptance-averaged (W, Q^2) in the response functions and found that it is sufficient to employ a dipole form factor to project $\overline{Q^2}$ to central kinematics. This bin-centering procedure reduces nonstatistical scatter in the data but has relatively little effect upon fitted multipole amplitudes.

Our primary analysis minimizes bias by using a pseudovector Born baseline model for $\ell > 2$ partial waves. Good fits are obtained by fitting all amplitudes for $\ell \leq 1$, but variation of all $\ell \leq 2$ amplitudes gives too much freedom and results in large uncertainties and strong correlations among parameters. Our final results vary Re $2-$ amplitudes in addition to all $\ell \leq 1$ amplitudes except Im M_{1-}; models predict that Im M_{1-} is negligible across our W range and its omission eliminates a troublesome correlation with Im S_{1-}. This truncation scheme permits more than the minimum required freedom without venturing into anarchy. Under these conditions the fitted amplitudes are rather insensitive to the choice of baseline model — although relatively strong d-wave amplitudes in SAID appear to adversely affect fits based upon that model, fits based upon MAID2003, DMT, or SL produce results very similar to those obtained with the Born baseline. Therefore, we judge the fitted multipole amplitudes and quadrupole ratios to be nearly model independent. Using a parabolic fit to the energy dependence, we obtain Re $(S_{1+}^{(p\pi^0)}/M_{1+}^{(p\pi^0)}) = -(6.61 \pm 0.18)\%$ and Re $(E_{1+}^{(p\pi^0)}/M_{1+}^{(p\pi^0)}) = -(2.87 \pm 0.19)\%$ at $W = M_\Delta = 1.232$ GeV and $Q^2 = 1.0$ (GeV/c)^2. The observation that traditional Legendre analysis of the same data produces significantly smaller quadrupole ratios demonstrates that its truncation is inadequate and that reliable results require a more complete multipole analysis.

---

[1] J. J. Kelly *et al.*, www.physics.umd.edu/enp/jjkelly/e91011/Reports/Publications/Drafts/ndel%ta_prc.ps.gz (unpublished).
[2] J. J. Kelly and T. M. Payerle, www.physics.umd.edu/enp/jjkelly/EPIPROD.
[3] J. J. Kelly and O. Gayou, www.physics.umd.edu/enp/jjkelly/e91011/Reports/Analysis/pseudodata_anal%ysis.ps.gz (unpublished).
[4] D. Drechsel, O. Hanstein, S. S. Kamalov, L. Tiator, and S. N. Yang, www.kph.uni-mainz.de/MAID.
[5] D. Drechsel, O. Hanstein, S. S. Kamalov, L. Tiator, and S. N. Yang, www.kph.uni-mainz.de/maid/dmt.
[6] R. A. Arndt, W. J. Briscoe, R. L. Workman, and I. I. Strakovsky, gwdac.phys.gwu.edu.
[7] T. Sato and T.-S. H. Lee, Phys. Rev. **C 63**, 055201 (2001).
[8] J. J. Kelly and O. Gayou, www.physics.umd.edu/enp/jjkelly/e91011/Reports/Analysis/syserr.ps.gz (unpublished).
[9] S. Escoffier, Ph.D. thesis, University of Paris, 2001.
[10] V. Punjabi *et al.*, Phys. Rev. **C 71**, 055202 (2005).
[11] L. Pentchev, JLAB-TN-03-024 (unpublished).
[12] I. G. Aznauryan, V. D. Burkert, H. Egiyan, K. Joo, R. Minehart, and L. C. Smith, Phys. Rev. **C 71**, 015201 (2005).
[13] K. Joo *et al.*, Phys. Rev. Lett. **88**, 122001 (2002).
[14] J. J. Kelly, www.physics.umd.edu/enp/jjkelly/e91011/Reports/Analysis/legendre.ps.gz (unpublished).
[15] J. J. Kelly, arXiv:nucl-ex/0705010 (unpublished).
[16] J. J. Kelly *et al.*, arXiv:nucl-ex/0505024 (unpublished).